



Pathway Analysis Report

This report contains the pathway analysis results for the submitted sample ". Analysis was performed against Reactome version 95 on 10/12/2025. The web link to these results is:

<https://reactome.org/PathwayBrowser/#/ANALYSIS=MjAyNTEyMTAxODU5MDJfMjM2Ng%3D%3D>

Please keep in mind that analysis results are temporarily stored on our server. The storage period depends on usage of the service but is at least 7 days. As a result, please note that this URL is only valid for a limited time period and it might have expired.

Table of Contents

1. Introduction
2. Properties
3. Genome-wide overview
4. Most significant pathways
5. Pathways details
6. Identifiers found
7. Identifiers not found

1. Introduction

Reactome is a curated database of pathways and reactions in human biology. Reactions can be considered as pathway 'steps'. Reactome defines a 'reaction' as any event in biology that changes the state of a biological molecule. Binding, activation, translocation, degradation and classical biochemical events involving a catalyst are all reactions. Information in the database is authored by expert biologists, entered and maintained by Reactome's team of curators and editorial staff. Reactome content frequently cross-references other resources e.g. NCBI, Ensembl, UniProt, KEGG (Gene and Compound), ChEBI, PubMed and GO. Orthologous reactions inferred from annotation for *Homo sapiens* are available for 14 non-human species including mouse, rat, chicken, puffer fish, worm, fly and yeast. Pathways are represented by simple diagrams following an SBGN-like format.

Reactome's annotated data describe reactions possible if all annotated proteins and small molecules were present and active simultaneously in a cell. By overlaying an experimental dataset on these annotations, a user can perform a pathway over-representation analysis. By overlaying quantitative expression data or time series, a user can visualize the extent of change in affected pathways and its progression. A binomial test is used to calculate the probability shown for each result, and the p-values are corrected for the multiple testing (Benjamini–Hochberg procedure) that arises from evaluating the submitted list of identifiers against every pathway.

To learn more about our Pathway Analysis, please have a look at our relevant publications:

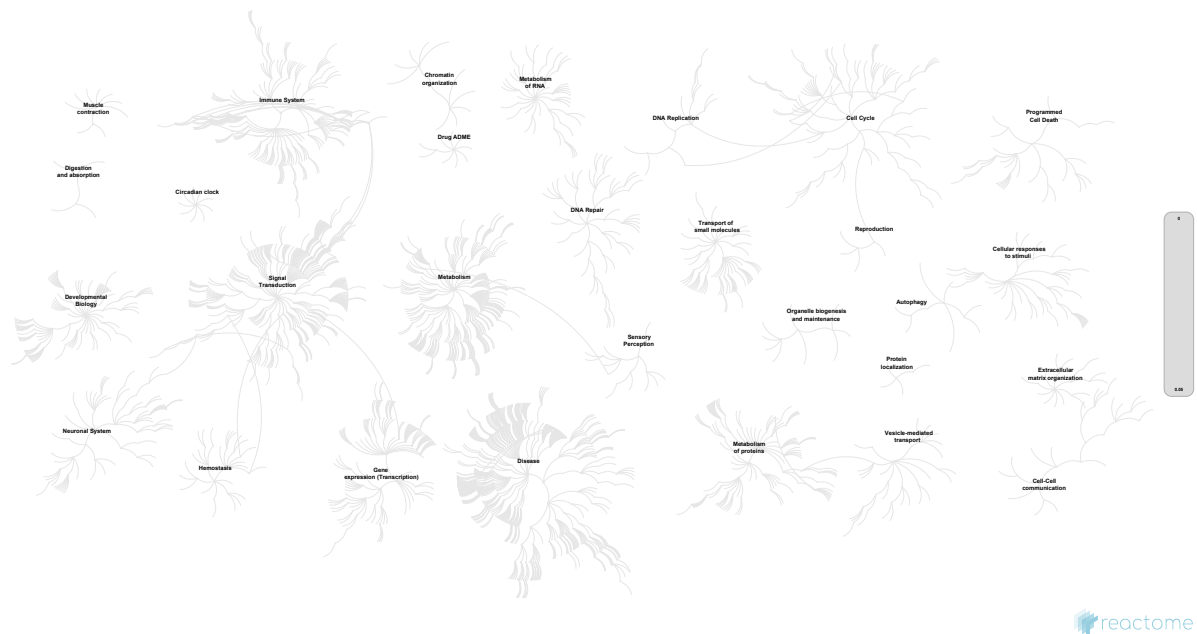
Fabregat A, Sidiropoulos K, Garapati P, Gillespie M, Hausmann K, Haw R, ... D'Eustachio P (2016). The reactome pathway knowledgebase. *Nucleic Acids Research*, 44(D1), D481–D487. <https://doi.org/10.1093/nar/gkv1351>. 

Fabregat A, Sidiropoulos K, Viteri G, Forner O, Marin-Garcia P, Arnau V, ... Hermjakob H (2017). Reactome pathway analysis: a high-performance in-memory approach. *BMC Bioinformatics*, 18. 

2. Properties

- This is an **overrepresentation** analysis: A statistical (hypergeometric distribution) test that determines whether certain Reactome pathways are over-represented (enriched) in the submitted data. It answers the question 'Does my list contain more proteins for pathway X than would be expected by chance?' This test produces a probability score, which is corrected for false discovery rate using the Benjamani-Hochberg method. ↗
- 593 out of 1482 identifiers in the sample were found in Reactome, where 2156 pathways were hit by at least one of them.
- All non-human identifiers have been converted to their human equivalent. ↗
- IntAct interactors were included to increase the analysis background. This greatly increases the size of Reactome pathways, which maximises the chances of matching your submitted identifiers to the expanded pathway, but will include interactors that have not undergone manual curation by Reactome and may include interactors that have no biological significance, or unexplained relevance.
- This report is filtered to show only results for species 'Homo sapiens' and resource 'all resources'.
- The unique ID for this analysis (token) is MjAyNTEyMTAxODU5MDJfMjM2Ng%3D%3D. This ID is valid for at least 7 days in Reactome's server. Use it to access Reactome services with your data.

3. Genome-wide overview



 reactome

This figure shows a genome-wide overview of the results of your pathway analysis. Reactome pathways are arranged in a hierarchy. The center of each of the circular "bursts" is the root of one top-level pathway, for example "DNA Repair". Each step away from the center represents the next level lower in the pathway hierarchy. The color code denotes over-representation of that pathway in your input dataset. Light grey signifies pathways which are not significantly over-represented.

4. Most significant pathways

The following table shows the 25 most relevant pathways sorted by p-value.

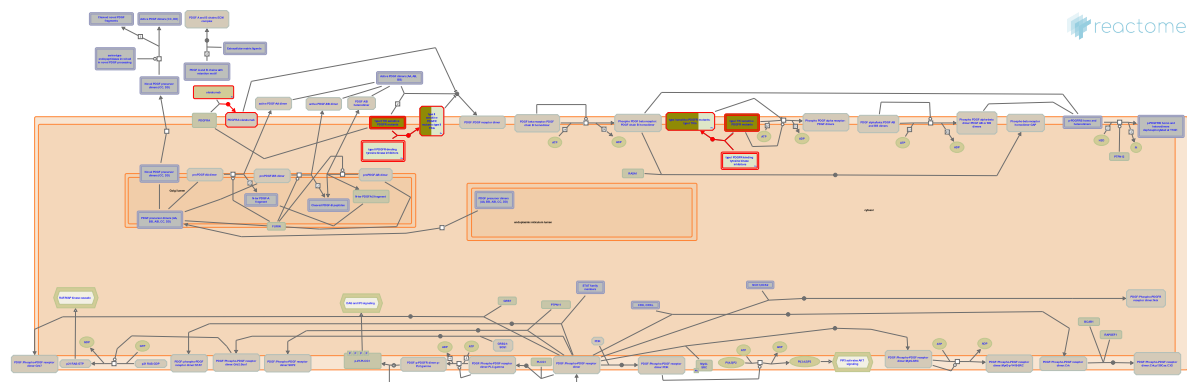
Pathway name	Entities				Reactions	
	found	ratio	p-value	FDR*	found	ratio
PDGFR mutants bind TKIs	1 / 1	4.03e-05	0.081	1	2 / 2	1.26e-04
Imatinib-resistant PDGFR mutants	1 / 1	4.03e-05	0.081	1	1 / 1	6.30e-05
Sorafenib-resistant PDGFR mutants	1 / 1	4.03e-05	0.081	1	1 / 1	6.30e-05
Signaling by MAP2K mutants	2 / 6	2.42e-04	0.092	1	1 / 1	6.30e-05
Translesion synthesis by POLK	5 / 23	9.26e-04	0.132	1	3 / 3	1.89e-04
APOBEC3G mediated resistance to HIV-1 infection	3 / 15	6.04e-04	0.134	1	3 / 3	1.89e-04
Anchoring fibril formation	3 / 15	6.04e-04	0.134	1	2 / 4	2.52e-04
MAP2K and MAPK activation	7 / 51	0.002	0.143	1	12 / 12	7.56e-04
Signaling by LTK in cancer	4 / 16	6.44e-04	0.154	1	3 / 4	2.52e-04
TGFBR2 MSI Frameshift Mutants in Cancer	1 / 2	8.06e-05	0.155	1	1 / 1	6.30e-05
Keratan sulfate degradation	4 / 25	0.001	0.162	1	3 / 7	4.41e-04
Signaling by high-kinase activity BRAF mutants	6 / 44	0.002	0.171	1	4 / 6	3.78e-04
Highly sodium permeable postsynaptic acetylcholine nicotinic receptors	2 / 9	3.62e-04	0.176	1	2 / 2	1.26e-04
Defective CYP11A1 causes AICSR	2 / 9	3.62e-04	0.176	1	1 / 1	6.30e-05
Acyl chain remodelling of PG	4 / 26	0.001	0.179	1	4 / 10	6.30e-04
Gap-filling DNA repair synthesis and ligation in GG-NER	4 / 27	0.001	0.195	1	2 / 2	1.26e-04
Electron transport from NADPH to Ferredoxin	2 / 10	4.03e-04	0.206	1	1 / 2	1.26e-04
PTEN Loss of Function in Cancer	1 / 3	1.21e-04	0.223	1	1 / 1	6.30e-05
MPS IV - Morquio syndrome B (CS/DS degradation)	1 / 3	1.21e-04	0.223	1	1 / 1	6.30e-05
MPS IV - Morquio syndrome B (Keratin metabolism)	1 / 3	1.21e-04	0.223	1	1 / 1	6.30e-05
RHOV GTPase cycle	5 / 39	0.002	0.234	1	1 / 2	1.26e-04
Signaling by RAF1 mutants	6 / 49	0.002	0.235	1	7 / 7	4.41e-04
RSK activation	2 / 11	4.43e-04	0.237	1	1 / 4	2.52e-04
RNA Polymerase II Transcription Initiation	6 / 50	0.002	0.249	1	3 / 3	1.89e-04
CS/DS degradation	5 / 40	0.002	0.25	1	4 / 12	7.56e-04

* False Discovery Rate

5. Pathways details

For every pathway of the most significant pathways, we present its diagram, as well as a short summary, its bibliography and the list of inputs found in it.

1. PDGFR mutants bind TKIs (R-HSA-9674428)



Diseases: cancer.

Aberrant signaling by activated forms of PDGFR can be inhibited by tyrosine kinase inhibitors (TKIs). PDGF receptors are class III receptor tyrosine kinase receptors, also known as dual-switch. Dual-switch receptors are activated through a series of phosphorylation and conformational changes that move the receptor from the inactive form to the fully activated form. Type II TKIs bind to the inactive form of the receptor at a site adjacent to the ATP-binding cleft, while type I TKIs bind to the active form (reviewed in Roskoski, 2018; Klug et al, 2018).

Primary mutations in PDGRFA occur in the activation loop, with a minor fraction found in the juxtamembrane domain (reviewed in Roskoski, 2018; Klug et al, 2018). Juxtamembrane domain mutations affect an autoinhibitory loop, shifting the equilibrium of the receptor towards the activated state; despite this, however, juxtamembrane domain mutants remain predominantly in the inactive state and as such are susceptible to inhibition by type II TKIs. Activation loop mutations more strongly favor the active conformation of the receptor and are susceptible to inhibition by both type II and type I TKI. The most prevalent PDGFRA mutation, D842V, promotes the active conformation strongly enough to be resistant to type II TKIs (reviewed in Roskoski, 2018; Klug et al, 2018).

References

- Roskoski R (2018). The role of small molecule platelet-derived growth factor receptor (PDGFR) inhibitors in the treatment of neoplastic disorders. *Pharmacol. Res.*, 129, 65-83. [🔗](#)
- Klug LR, Kent JD & Heinrich MC (2018). Structural and clinical consequences of activation loop mutations in class III receptor tyrosine kinases. *Pharmacol. Ther.*, 191, 123-134. [🔗](#)

Edit history

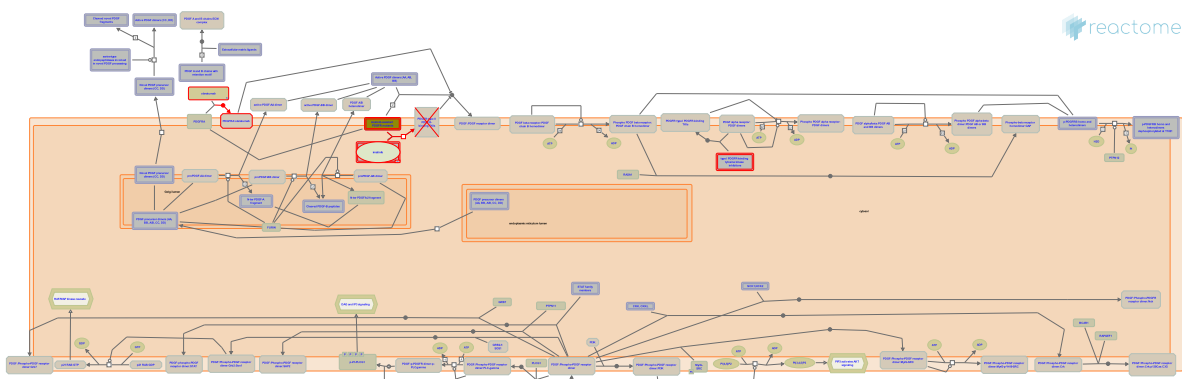
Date	Action	Author
2020-01-13	Created	Rothfels K
2020-02-06	Reviewed	Ip CKM
2020-02-25	Edited	Rothfels K

Date	Action	Author
2020-02-25	Authored	Rothfels K
2023-03-08	Modified	Matthews L

1 submitted entities found in this pathway, mapping to 1 Reactome entities

Input	UniProt Id
PDGFRA	P16234

2. Imatinib-resistant PDGFR mutants (R-HSA-9674396)



Diseases: cancer.

A number of PDGFRA mutations found in GIST and other cancers are resistant to inhibition with imatinib (reviewed in Corless et al, 2011). These include the most common allele D842V, which occurs in the activation loop of the receptor, as well as S601P and the gatekeeper mutation T674I (re-reviewed in Roskoski, 2018; Klug et al, 2018).

References

- Corless CL, Barnett CM & Heinrich MC (2011). Gastrointestinal stromal tumours: origin and molecular oncology. *Nat. Rev. Cancer*, 11, 865-78. [🔗](#)
- Roskoski R (2018). The role of small molecule platelet-derived growth factor receptor (PDGFR) inhibitors in the treatment of neoplastic disorders. *Pharmacol. Res.*, 129, 65-83. [🔗](#)
- Klug LR, Kent JD & Heinrich MC (2018). Structural and clinical consequences of activation loop mutations in class III receptor tyrosine kinases. *Pharmacol. Ther.*, 191, 123-134. [🔗](#)

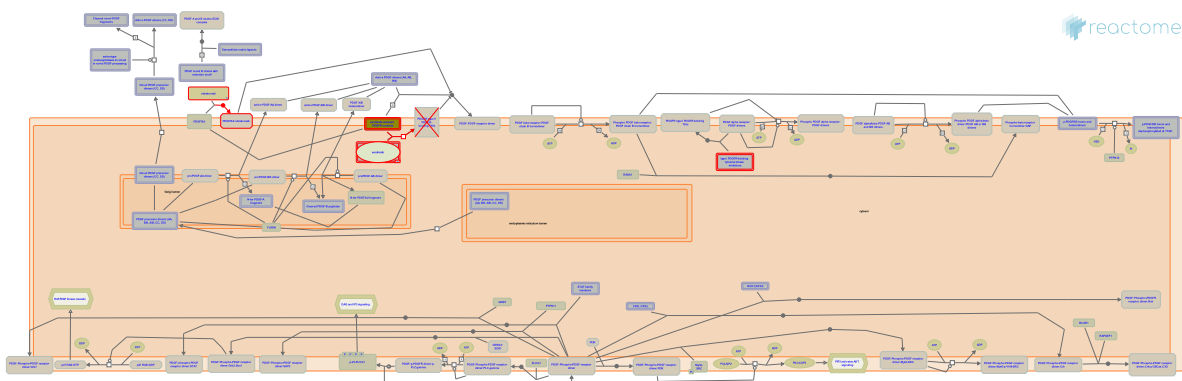
Edit history

Date	Action	Author
2020-01-13	Created	Rothfels K
2020-02-06	Reviewed	Ip CKM
2020-02-25	Edited	Rothfels K
2020-02-25	Authored	Rothfels K
2023-03-08	Modified	Matthews L

1 submitted entities found in this pathway, mapping to 1 Reactome entities

Input	UniProt Id
PDGFRA	P16234

3. Sorafenib-resistant PDGFR mutants (R-HSA-9674404)



Diseases: cancer.

Sorafenib is a type II tyrosine kinase inhibitor that is approved for use in hepatocellular and renal cell carcinoma, and that is often used as a second-line treatment for imatinib-resistant tumors. Despite its initial efficacy, resistance to sorafenib often develops (reviewed in Molina-Ruiz et al, 2017).

References

- Corless CL, Barnett CM & Heinrich MC (2011). Gastrointestinal stromal tumours: origin and molecular oncology. *Nat. Rev. Cancer*, 11, 865-78. [View](#)
- Molina-Ruiz FJ, Gonzalez R, Rodriguez-Hernandez MA, Navarro-Villaran E, Padillo FJ & Muntané J (2016). Antitumoral Activity of Sorafenib in Hepatocellular Carcinoma: Effects on Cell Survival and Death Pathways, Cell Metabolism Reprogramming, and Nitrosative and Oxidative Stress. *Crit Rev Oncog*, 21, 413-432. [View](#)

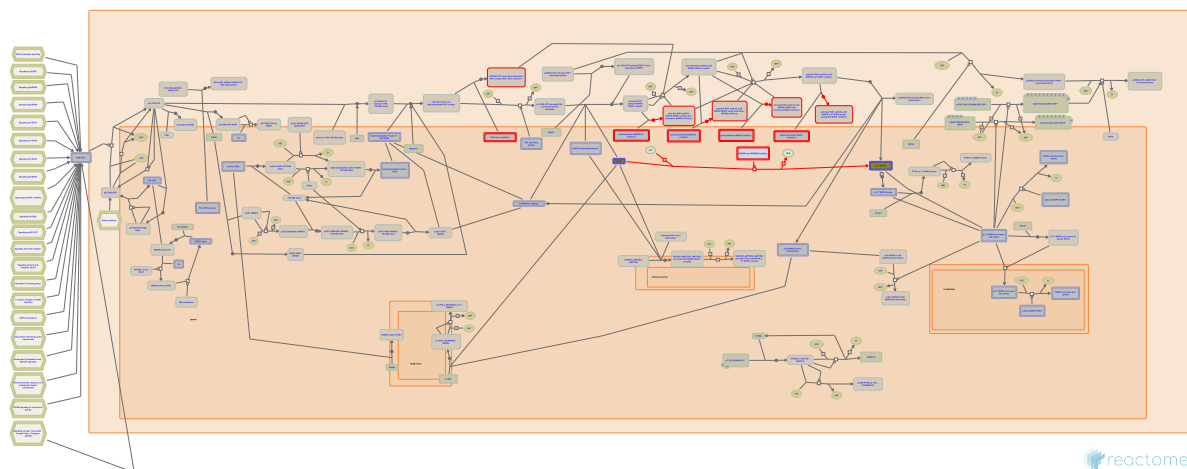
Edit history

Date	Action	Author
2020-01-13	Created	Rothfels K
2020-02-06	Reviewed	Ip CKM
2020-02-25	Edited	Rothfels K
2020-02-25	Authored	Rothfels K
2023-03-08	Modified	Matthews L

1 submitted entities found in this pathway, mapping to 1 Reactome entities

Input	UniProt Id
PDGFRA	P16234

4. Signaling by MAP2K mutants (R-HSA-9652169)



Diseases: cancer, cardiofaciocutaneous syndrome.

Activating mutations in MAP2K1 and MAP2K2, the genes encoding MEK1 and MEK2, have been identified at low frequency in a variety of cancers as well as in germline diseases such as Noonan syndrome, cardiofaciocutaneous syndromes and other RASopathies (reviewed in Samatar and Poulikakos, 2014; Bezniakow et al, 2014; Rauen, 2013).

References

- Samatar AA & Poulikakos PI (2014). Targeting RAS-ERK signalling in cancer: promises and challenges. *Nat Rev Drug Discov*, 13, 928-42. [\[link\]](#)
- Bezniakow N, Gos M & Obersztyn E (2014). The RASopathies as an example of RAS/MAPK pathway disturbances - clinical presentation and molecular pathogenesis of selected syndromes. *Dev Period Med*, 18, 285-96. [\[link\]](#)
- Rauen KA (2013). The RASopathies. *Annu Rev Genomics Hum Genet*, 14, 355-69. [\[link\]](#)

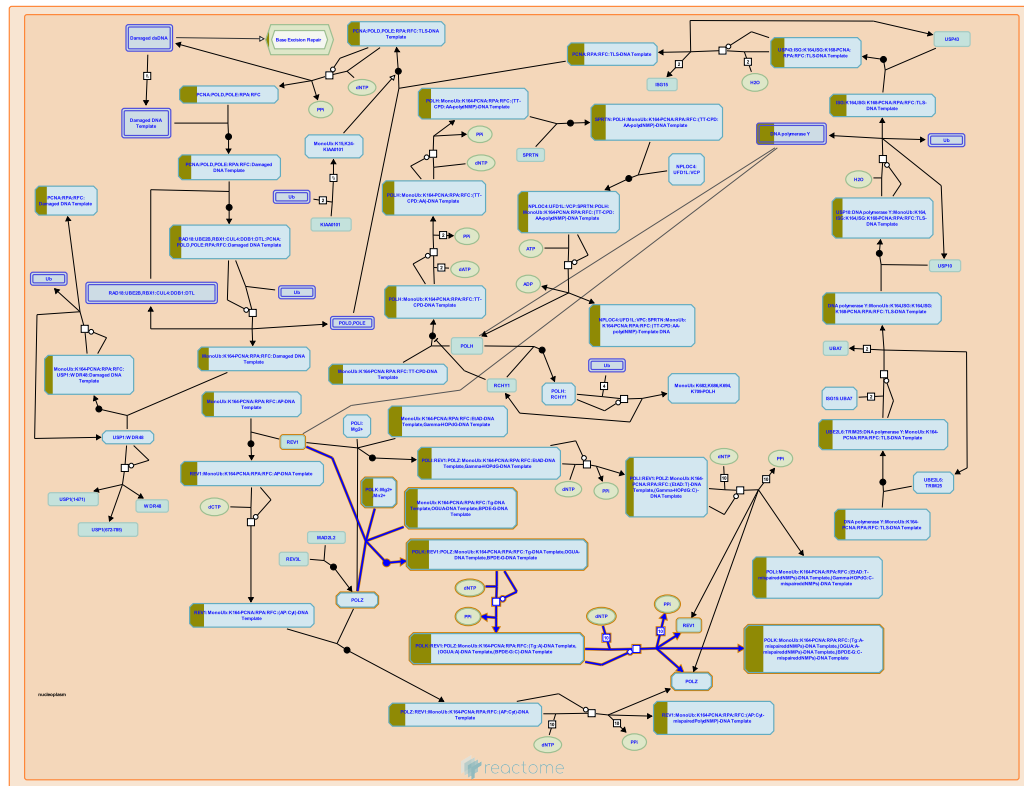
Edit history

Date	Action	Author
2019-06-27	Created	Rothfels K
2019-10-25	Authored	Rothfels K
2020-05-04	Reviewed	Gavathiotis E
2020-05-26	Edited	Rothfels K

1 submitted entities found in this pathway, mapping to 2 Reactome entities

Input	UniProt Id
MAPK3	P27361, P28482

5. Translesion synthesis by POLK (R-HSA-5655862)



Cellular compartments: nucleoplasm.

DNA polymerase kappa (POLK) is a Y family DNA polymerase that is most efficient in translesion DNA synthesis (TLS) across oxidation derivatives of DNA bases, such as thymine glycol (Tg) and 8-oxoguanine (OGUA), as well as bulky DNA adducts, such as benzo(a)pyrene diol epoxide guanine adduct (BPDE-G) (Zhang et al. 2000, Fischhaber et al. 2002, Avkin et al. 2004, Vasquez-Del Carpio et al. 2009, Yoon et al. 2010, Lior-Hoffmann et al. 2012, Christov et al. 2012, Yoon et al. 2014). POLK carries out TLS by forming a quaternary complex with REV1 and monoubiquitinated PCNA (Ohashi et al. 2009, Haracska, Unk et al. 2002, Bi et al. 2006). POLK and POLZ cooperate in the elongation of nucleotides inserted opposite to lesioned bases by POLK. Similarly to POLZ, POLK has low processivity and is error-prone (Ohashi et al. 2000, Haracska, Prakash et al. 2002, Yoon et al. 2010).

References

- Ohashi E, Hanafusa T, Kamei K, Song I, Tomida J, Hashimoto H, ... Ohmori H (2009). Identification of a novel REV1-interacting motif necessary for DNA polymerase kappa function. *Genes Cells*, 14, 101-11. [🔗](#)
- Haracska L, Unk I, Johnson RE, Phillips BB, Hurwitz J, Prakash L & Prakash S (2002). Stimulation of DNA synthesis activity of human DNA polymerase kappa by PCNA. *Mol. Cell. Biol.*, 22, 784-91. [🔗](#)
- Fischhaber PL, Gerlach VL, Feaver WJ, Hatahet Z, Wallace SS & Friedberg EC (2002). Human DNA polymerase kappa bypasses and extends beyond thymine glycols during translesion synthesis in vitro, preferentially incorporating correct nucleotides. *J. Biol. Chem.*, 277, 37604-11. [🔗](#)
- Yoon JH, Roy Choudhury J, Park J, Prakash S & Prakash L (2014). A role for DNA polymerase ? in promoting replication through oxidative DNA lesion, thymine glycol, in human cells. *J. Biol. Chem.*, 289, 13177-85. [🔗](#)

Yoon JH, Bhatia G, Prakash S & Prakash L (2010). Error-free replicative bypass of thymine glycol by the combined action of DNA polymerases kappa and zeta in human cells. Proc. Natl. Acad. Sci. U.S.A., 107, 14116-21. 

Edit history

Date	Action	Author
2014-12-09	Created	Orlic-Milacic M
2014-12-11	Edited	Orlic-Milacic M
2014-12-11	Authored	Orlic-Milacic M
2015-01-07	Reviewed	Borowiec JA

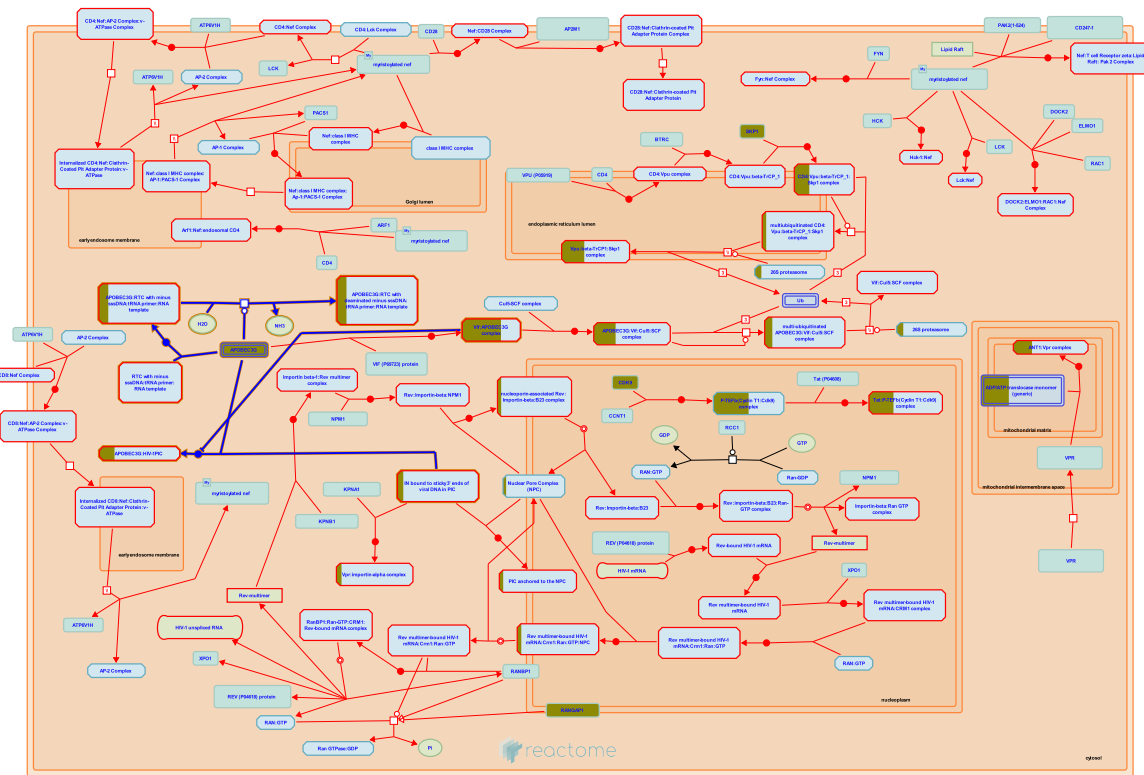
3 submitted entities found in this pathway, mapping to 4 Reactome entities

Input	UniProt Id	Input	UniProt Id	Input	UniProt Id
POLK	Q9UBT6	RFC4	P35249, P35250	RPA3	P35244

Interactors found in this pathway (1)

Input	UniProt Id	Interacts with	Input	UniProt Id	Interacts with
FHL2	Q14192	Q9UBZ9			

6. APOBEC3G mediated resistance to HIV-1 infection ([R-HSA-180689](#))



Diseases: Human immunodeficiency virus infectious disease.

Representatives of the apolipoprotein B mRNA editing enzyme catalytic polypeptide 3 (APOBEC3) family provide innate resistance to exogenous and endogenous retroviruses (see Cullen 2006 for a recent review). Humans and other primates encode a cluster of seven different cytidine deaminases with APOBEC3G, APOBEC3F and APOBEC3B having some anti HIV-1 activity. Our understanding is most complete for APOBEC3G which has been described first and the reactions described herein will focus on this representative enzyme.

APOBEC3G is a cytoplasmic protein which strongly restricts replication of Vif deficient HIV-1 (Sheehy 2002). It is expressed in cell populations that are susceptible to HIV infection (e.g., T-lymphocytes and macrophages). In the producer cell, APOBEC3G is incorporated into budding HIV-1 particles through an interaction with HIV-1 gag nucleocapsid (NC) protein in a RNA-dependent fashion.

Within the newly infected cell (= target cell), virus-associated APOBEC3G regulates the infectivity of HIV-1 by deaminating cytidine to uracil in the minus-strand viral DNA intermediate during reverse transcription. Deamination results in the induction of G-to-A hypermutations in the plus-strand viral DNA which subsequently can either be integrated as a non-functional provirus or degraded before integration.

References

Cullen BR (2006). Role and mechanism of action of the APOBEC3 family of antiretroviral resistance factors. *J Virol*. 80, 1067-76.

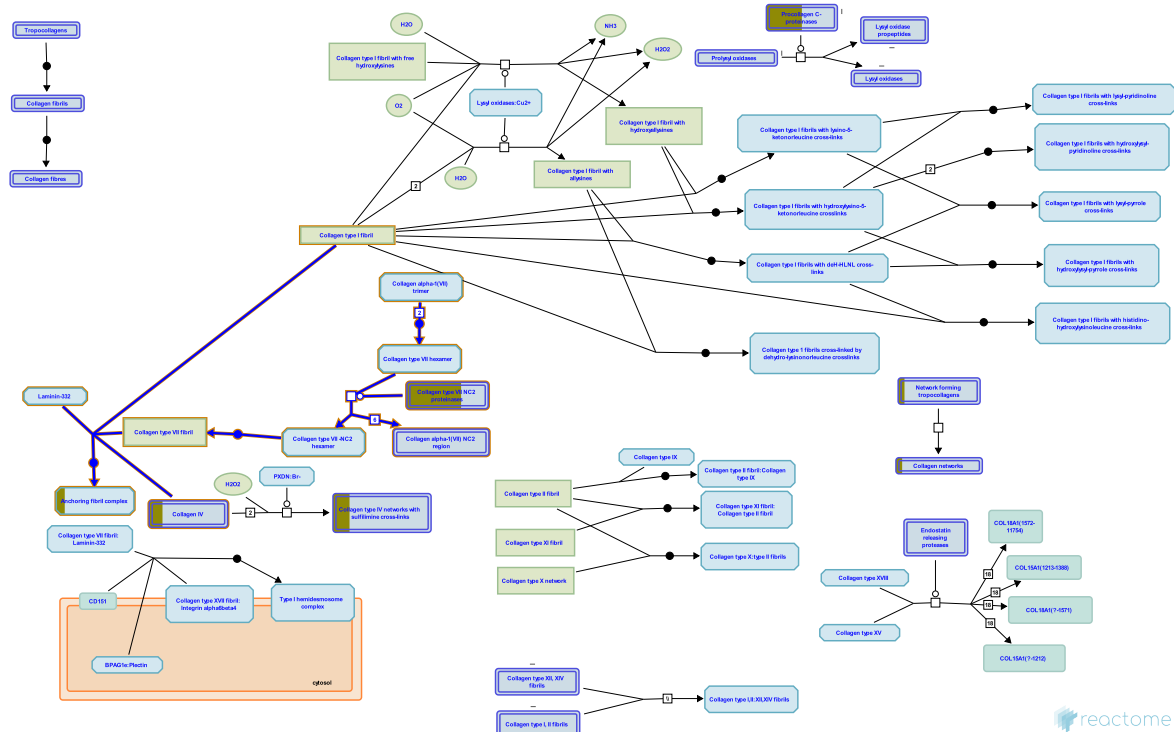
Edit history

Date	Action	Author
2006-06-02	Created	Matthews L
2006-06-08	Authored	Matthews L
2007-01-30	Edited	Matthews L
2007-01-31	Reviewed	Mulder L, Simon V
2023-10-12	Modified	Weiser JD

2 submitted entities found in this pathway, mapping to 3 Reactome entities

Input	UniProt Id	Input	UniProt Id
APOBEC3G	Q9HC16-1, Q9HC16-3	BANF1	O75531

7. Anchoring fibril formation (R-HSA-2214320)



Cellular compartments: extracellular region.

Collagen VII forms anchoring fibrils, composed of antiparallel dimers that connect the dermis to the epidermis (Bruckner-Tuderman 2009, Has & Kern 2010). During fibrillogenesis, the nascent type VII procollagen molecules dimerize in an antiparallel manner. The C-propeptide is then removed by Bone morphogenetic protein 1 (Rattenholl et al. 2002) and the processed antiparallel dimers laterally aggregate (Villone et al. 2008, Gordon & Hahn 2010).

References

Chung HJ & Uitto J (2010). Type VII collagen: the anchoring fibril protein at fault in dystrophic epidermolysis bullosa. Dermatol Clin, 28, 93-105. [\[link\]](#)

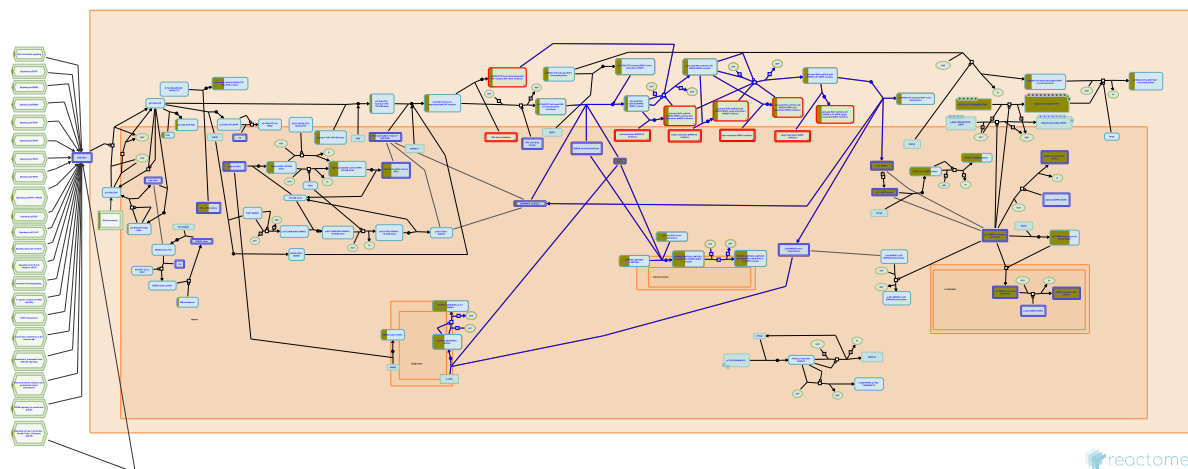
Edit history

Date	Action	Author
2012-04-30	Authored	Jupe S
2012-04-30	Created	Jupe S
2012-10-08	Reviewed	Kalamajski S, Raleigh S
2012-11-12	Edited	Jupe S
2012-11-19	Reviewed	Ricard-Blum S
2025-11-15	Modified	Weiser JD

3 submitted entities found in this pathway, mapping to 3 Reactome entities

Input	UniProt Id	Input	UniProt Id	Input	UniProt Id
BMP1	P13497	COL4A3	Q01955	TLL1	O43897

8. MAP2K and MAPK activation (R-HSA-5674135)



Activated RAF proteins are restricted substrate kinases whose primary downstream targets are the two MAP2K proteins, MAP2K1 and MAP2K2 (also known as MEK1 and MEK2) (reviewed in Roskoski, 2010, Roskoski, 2012a). Phosphorylation of the MAP2K activation loop primes them to phosphorylate the primary effector of the activated MAPK pathway, the two MAPK proteins MAPK3 and MAPK1 (also known as ERK1 and 2). Unlike their upstream counterparts, MAPK3 and MAPK1 catalyze the phosphorylation of hundreds of cytoplasmic and nuclear targets including transcription factors and regulatory molecules (reviewed in Roskoski, 2012b). Activation of MAP2K and MAPK proteins downstream of activated RAF generally occurs in the context of a higher order scaffolding complex that regulates the specificity and localization of the pathway (reviewed in Brown and Sacks, 2009; Matallanas et al, 2011).

References

- Roskoski R Jr (2012). ERK1/2 MAP kinases: structure, function, and regulation. *Pharmacol. Res.*, 66, 105-43. [🔗](#)
- Roskoski R Jr (2012). MEK1/2 dual-specificity protein kinases: structure and regulation. *Biochem. Biophys. Res. Commun.*, 417, 5-10. [🔗](#)
- Roskoski R Jr (2010). RAF protein-serine/threonine kinases: structure and regulation. *Biochem. Biophys. Res. Commun.*, 399, 313-7. [🔗](#)
- Matallanas D, Birtwistle M, Romano D, Zebisch A, Rauch J, von Kriegsheim A & Kolch W (2011). Raf family kinases: old dogs have learned new tricks. *Genes Cancer*, 2, 232-60. [🔗](#)
- Brown MD & Sacks DB (2009). Protein scaffolds in MAP kinase signalling. *Cell. Signal.*, 21, 462-9. [🔗](#)

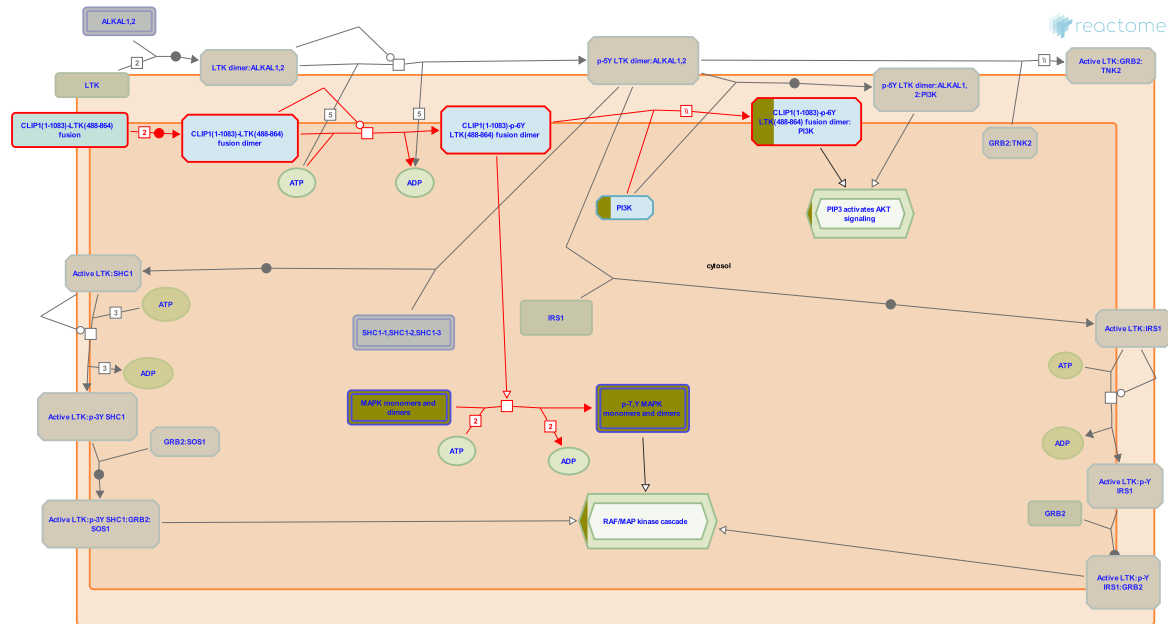
Edit history

Date	Action	Author
2015-02-10	Authored	Rothfels K
2015-02-11	Created	Rothfels K
2015-02-12	Edited	Rothfels K
2015-04-29	Reviewed	Roskoski R Jr

6 submitted entities found in this pathway, mapping to 7 Reactome entities

Input	UniProt Id	Input	UniProt Id	Input	UniProt Id
FGA	P02671	MAPK3	P27361, P28482	RAF1	P04049
RAP1A	P62834	VCL	P18206	WDR83	Q9BRX9

9. Signaling by LTK in cancer (R-HSA-9842640)



Diseases: cancer, non-small cell lung carcinoma.

LTK is a member of the anaplastic lymphoma kinase (ALK)/LTK subfamily within the insulin receptor superfamily of RTKs. LTK encodes an 864-amino-acid protein consisting of extracellular, transmembrane, and tyrosine kinase domains and a short carboxy terminus. The LTK kinase domain shares 80% identity with ALK (Roll and Reuther, 2012). The biological role of LTK is not well defined under normal physiological conditions, and unlike ALK, a clear role for LTK in cancer is also not yet well established. LTK is overexpressed in leukemia, and high expression of LTK in early-stage non-small cell lung cancer (NSCLC) has been associated with greater risk of metastasis (Mueller-Tidow et al, 2005; Roll and Reuther, 2012). More recently, a novel CLIP1-LTK fusion protein has been identified in a small proportion of NSCLC cases (Izumi et al, 2021).

References

- Roll JD & Reuther GW (2012). ALK-activating homologous mutations in LTK induce cellular transformation. PLoS One, 7, e31733. 

Müller-Tidow C, Diederichs S, Bulk E, Pohle T, Steffen B, Schwäble J, ... Serve H (2005). Identification of metastasis-associated receptor tyrosine kinases in non-small cell lung cancer. Cancer Res, 65, 1778-82. 

Izumi H, Matsumoto S, Liu J, Tanaka K, Mori S, Hayashi K, ... Goto K (2021). The CLIP1-LTK fusion is an oncogenic driver in non-small-cell lung cancer. Nature, 600, 319-323. 

Edit history

Date	Action	Author
2023-08-27	Created	Rothfels K
2023-10-14	Edited	Rothfels K
2023-10-14	Authored	Rothfels K
2024-03-04	Modified	Rothfels K

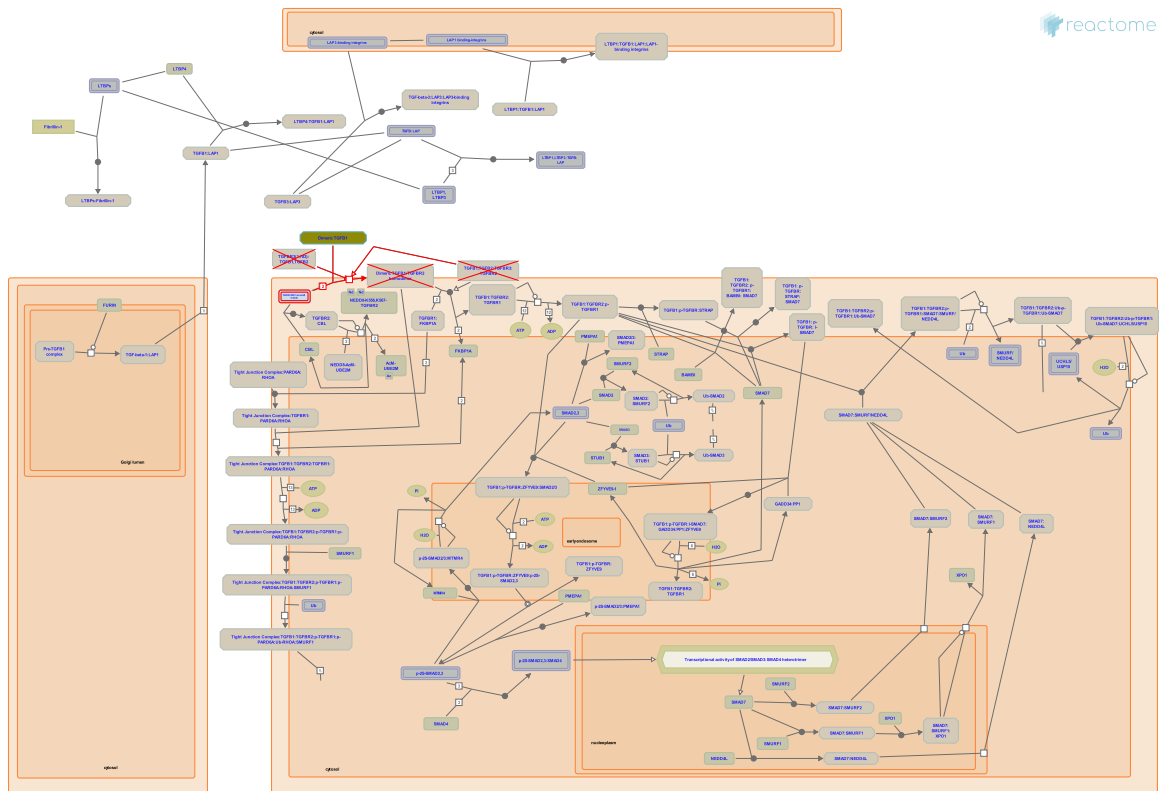
2 submitted entities found in this pathway, mapping to 3 Reactome entities

Input	UniProt Id	Input	UniProt Id
MAPK3	P27361, P28482	PIK3R1	P27986

Interactors found in this pathway (1)

Input	UniProt Id	Interacts with	Input	UniProt Id	Interacts with
REL	Q04864-2	P30622			

10. TGFBR2 MSI Frameshift Mutants in Cancer ([R-HSA-3642279](#))



Diseases: cancer.

The short adenine repeat in the coding sequence of TGF-beta receptor II (TGFBR2) gene is frequently targeted by loss-of-function frameshift mutations in colon cancers with microsatellite instability (MSI). The 1- or 2-bp deletions in the adenine stretch of TGFBR2 cDNA introduce a premature stop codon that leads to degradation of the majority of mutant transcripts through nonsense-mediated decay or to production of a truncated TGFBR2 that cannot be presented on the cell surface. Cells that harbor TGFBR2 MSI frameshift mutations are resistant to TGF-beta (TGFB1)-mediated growth inhibition.

References

- Markowitz S, Wang J, Myeroff L, Parsons R, Sun L, Lutterbaugh J, ... Vogelstein B (1995). Inactivation of the type II TGF-beta receptor in colon cancer cells with microsatellite instability. *Science*, 268, 1336-8. 

Wang J, Sun L, Myeroff L, Wang X, Gentry LE, Yang J, ... Willson JK (1995). Demonstration that mutation of the type II transforming growth factor beta receptor inactivates its tumor suppressor activity in replication error-positive colon carcinoma cells. *J. Biol. Chem.*, 270, 22044-9. 

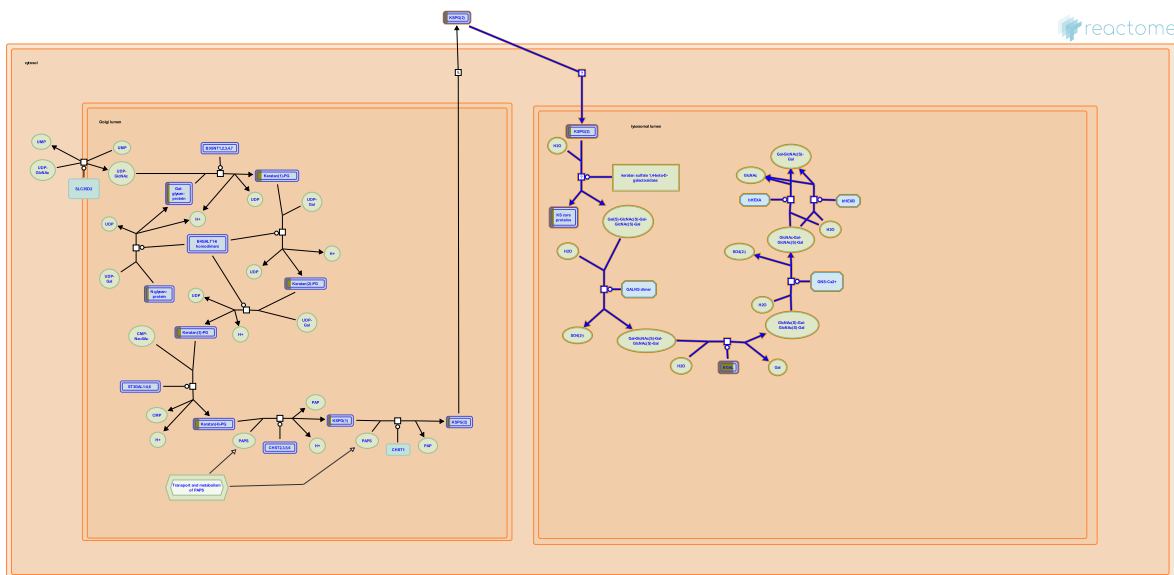
Edit history

Date	Action	Author
2013-05-30	Created	Orlic-Milacic M
2013-08-08	Edited	Orlic-Milacic M
2013-08-08	Reviewed	Meyer S, Akhurst RJ
2013-08-08	Authored	Meyer S, Akhurst RJ, Orlic-Milacic M

1 submitted entities found in this pathway, mapping to 1 Reactome entities

Input	UniProt Id
TGFB1	P01137

11. Keratan sulfate degradation (R-HSA-2022857)



Keratan sulfate proteoglycans (KSPGs) are degraded in lysosomes as part of normal homeostasis of glycoproteins. Glycoproteins must be completely degraded to avoid undigested fragments building up and causing a variety of lysosomal storage diseases. KSPGs are Asn-linked glycoproteins and are acted upon by exo-glycosidases to release sugar monomers. The main steps of degradation are shown representing the types of cleavage reactions that occur so the full degradation of KS is not shown to avoid repetition. The proteolysis of the core protein of the glycoprotein is not shown here (Winchester 2005, Aronson & Kuranda 1989).

References

- Winchester B (2005). Lysosomal metabolism of glycoproteins. *Glycobiology*, 15, 1R-15R. [🔗](#)

Aronson NN Jr & Kuranda MJ (1989). Lysosomal degradation of Asn-linked glycoproteins. *FASEB J*, 3, 2615-22. [🔗](#)

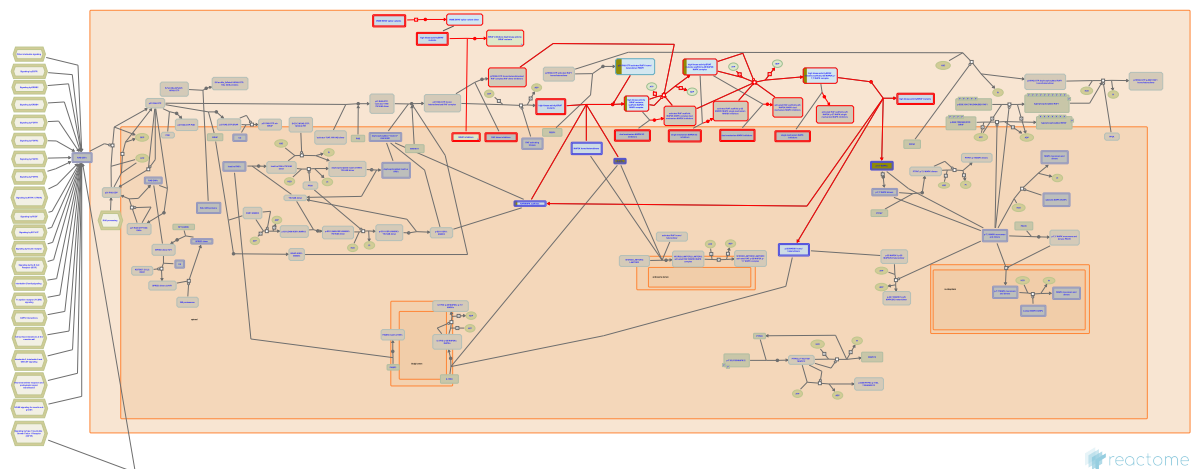
Edit history

Date	Action	Author
2011-12-01	Edited	Jassal B
2011-12-01	Authored	Jassal B
2011-12-01	Created	Jassal B
2012-03-28	Reviewed	D'Eustachio P
2025-11-15	Modified	Weiser J D

2 submitted entities found in this pathway, mapping to 4 Reactome entities

Input	UniProt Id	Input	UniProt Id
ACAN	P16112	GLB1	P16278, Q6UWU2, Q8NCI6

12. Signaling by high-kinase activity BRAF mutants (R-HSA-6802948)



Diseases: cancer.

BRAF is mutated in about 8% of human cancers, with high prevalence in hairy cell leukemia, melanoma, papillary thyroid and ovarian carcinomas, colorectal cancer and a variety of other tumors (Davies et al, 2002; reviewed in Samatar and Poulikakos, 2014). Most BRAF mutations fall in the activation loop region of the kinase or the adjacent glycine rich region. These mutations promote increased kinase activity either by mimicking the effects of activation loop phosphorylations or by promoting the active conformation of the enzyme (Davies et al, 2002; Wan et al, 2004). Roughly 90% of BRAF mutants are represented by the single missense mutation BRAF V600E (Davies et al, 2002; Wan et al, 2004). Other highly active kinase mutants of BRAF include BRAF G469A and BRAF T599dup. G469 is in the glycine rich region of the kinase domain which plays a role in orienting ATP for catalysis, while T599 is one of the two conserved regulatory phosphorylation sites of the activation loop. Each of these mutants has highly enhanced basal kinase activities, phosphorylates MEK and ERK in vitro and in vivo and is transforming when expressed in vivo (Davies et al, 2002; Wan et al, 2004; Eisenhardt et al, 2011). Further functional characterization shows that these highly active mutants are largely resistant to disruption of the BRAF dimer interface, suggesting that they are able to act as monomers (Roring et al, 2012; Brummer et al, 2006; Freeman et al, 2013; Garnett et al, 2005). Activating BRAF mutations occur for the most part independently of RAS activating mutations, and RAS activity levels are generally low in BRAF mutant cells. Moreover, the kinase activity of these mutants is only slightly elevated by coexpression of G12V KRAS, and biological activity of the highly active BRAF mutants is independent of RAS binding (Brummer et al, 2006; Wan et al, 2004; Davies et al, 2002; Garnett et al, 2005). Although BRAF V600E is inhibited by RAF inhibitors such as vemurafenib, resistance frequently develops, in some cases mediated by the expression of a splice variant that lacks the RAS binding domain and shows elevated dimerization compared to the full length V600E mutant (Poulikakos et al, 2011; reviewed in Lito et al, 2013).

References

- Davies H, Bignell GR, Cox C, Stephens P, Edkins S, Clegg S, ... Futreal PA (2002). Mutations of the BRAF gene in human cancer. *Nature*, 417, 949-54. [🔗](#)
- Samatar AA & Poulikakos PI (2014). Targeting RAS-ERK signalling in cancer: promises and challenges. *Nat Rev Drug Discov*, 13, 928-42. [🔗](#)

Wan PT, Garnett MJ, Roe SM, Lee S, Niculescu-Duvaz D, Good VM, ... Marais R (2004). Mechanism of activation of the RAF-ERK signaling pathway by oncogenic mutations of B-RAF. *Cell*, 116, 855-67. 

Eisenhardt AE, Olbrich H, Röring M, Janzarik W, Anh TN, Cin H, ... Brummer T (2011). Functional characterization of a BRAF insertion mutant associated with pilocytic astrocytoma. *Int. J. Cancer*, 129, 2297-303. 

Röring M, Herr R, Fiala GJ, Heilmann K, Braun S, Eisenhardt AE, ... Brummer T (2012). Distinct requirement for an intact dimer interface in wild-type, V600E and kinase-dead B-Raf signalling. *EMBO J.*, 31, 2629-47. 

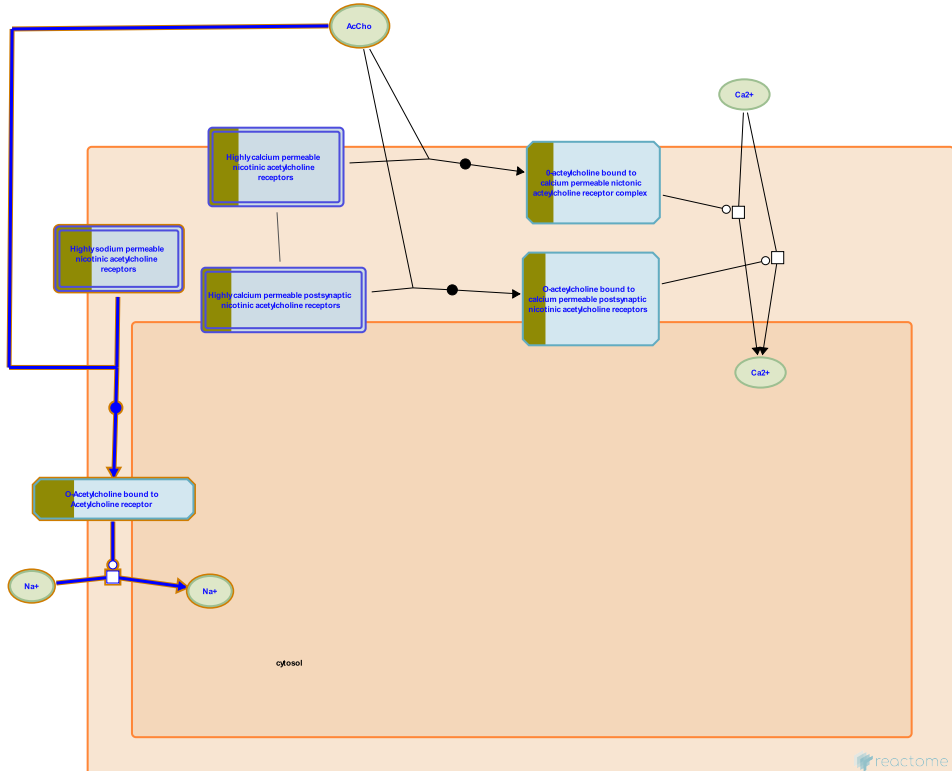
Edit history

Date	Action	Author
2015-08-10	Edited	Rothfels K
2015-08-10	Authored	Rothfels K
2015-10-02	Created	Rothfels K
2016-08-05	Reviewed	Stephens RM

5 submitted entities found in this pathway, mapping to 6 Reactome entities

Input	UniProt Id	Input	UniProt Id	Input	UniProt Id
FGA	P02671	MAPK3	P27361, P28482	RAF1	P04049
RAP1A	P62834	VCL	P18206		

13. Highly sodium permeable postsynaptic acetylcholine nicotinic receptors (R-HSA-629587)



Cellular compartments: cytosol, extracellular region, plasma membrane.

Nicotinic acetylcholine receptors that have low Ca²⁺ permeability allow the influx of Na⁺ which causes depolarization of the membrane initiating voltage dependent responses such as activation of voltage dependent opening of Ca²⁺ channels and thus eliciting an increase in Ca²⁺ and downstream signaling. These receptors could be found in both presynaptic and postsynaptic terminals.

References

Haass M & Kübler W (1997). Nicotine and sympathetic neurotransmission. Cardiovasc Drugs Ther, 10, 657-65. ↗

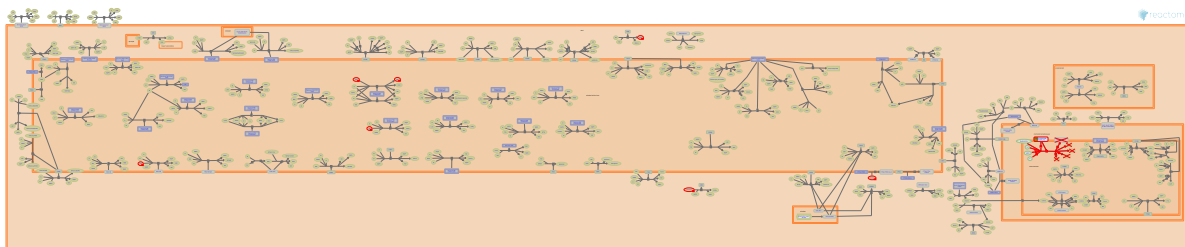
Edit history

Date	Action	Author
2008-11-27	Reviewed	Restituito S
2010-04-27	Authored	Mahajan SS
2010-04-27	Created	Mahajan SS
2010-05-19	Edited	Gillespie ME
2020-01-24	Reviewed	Wen H
2025-11-15	Modified	Weiser JD

2 submitted entities found in this pathway, mapping to 2 Reactome entities

Input	UniProt Id	Input	UniProt Id
CHRNA3	P32297	CHRNA4	P43681

14. Defective CYP11A1 causes AICSR (R-HSA-5579026)



Diseases: congenital adrenal insufficiency.

Cholesterol side-chain cleavage enzyme, mitochondrial (CYP11A1) normally catalyses the side-chain cleavage of cholesterol to form pregnenolone. Defects in CYP11A1 can cause Adrenal insufficiency, congenital, with 46,XY sex reversal (AICSR; MIM:613743). This is a rare disorder that can present as acute adrenal insufficiency in infancy with elevated ACTH and plasma renin activity and low or absent adrenal steroids. The severest phenotype is loss-of-function mutations associated with prematurity, complete under-androgenisation and severe, early-onset adrenal failure (Kim et al. 2008).

References

Kim CJ, Lin L, Huang N, Quigley CA, AvRuskin TW, Achermann JC & Miller WL (2008). Severe combined adrenal and gonadal deficiency caused by novel mutations in the cholesterol side chain cleavage enzyme, P450scc. *J. Clin. Endocrinol. Metab.*, 93, 696-702. [View](#)

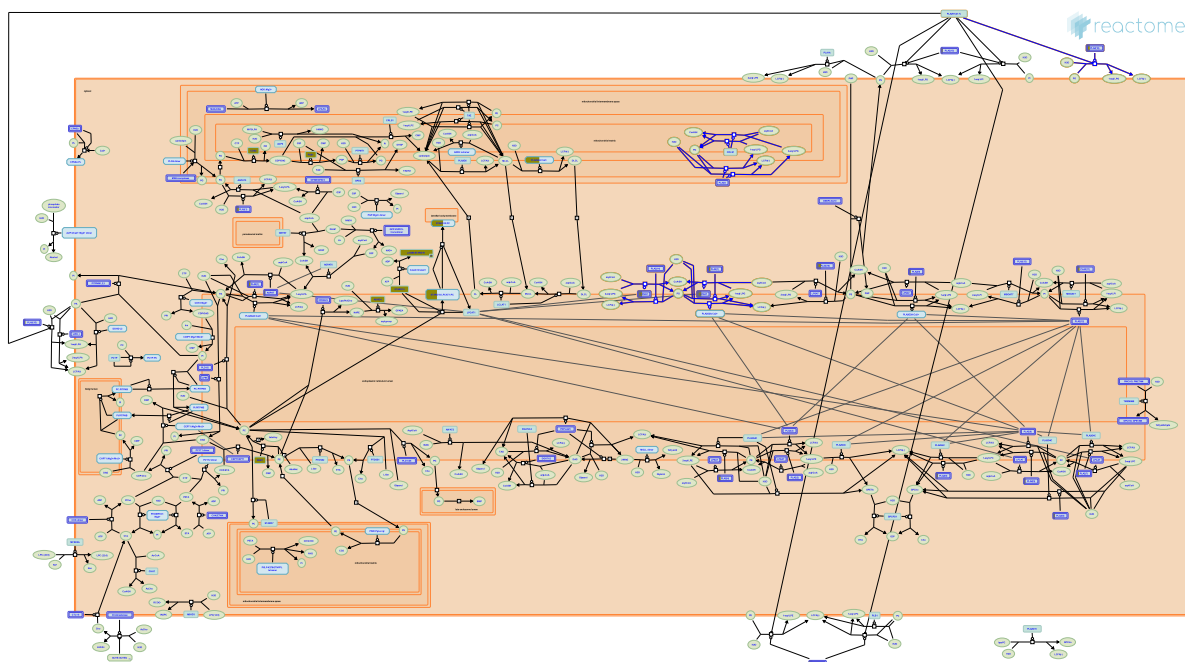
Edit history

Date	Action	Author
2014-06-06	Edited	Jassal B
2014-06-06	Authored	Jassal B
2014-06-06	Created	Jassal B
2014-11-03	Reviewed	Nakaki T
2023-10-12	Modified	Weiser JD

1 submitted entities found in this pathway, mapping to 2 Reactome entities

Input	UniProt Id
FDX1	P10109, Q6P4F2

15. Acyl chain remodelling of PG (R-HSA-1482925)



In the acyl chain remodelling pathway (Lands cycle), phosphatidylglycerol (PG) is hydrolyzed by phospholipases and subsequently reacylated by acyltransferases. These cycles modify the fatty acid composition of glycerophospholipids to generate diverse molecules asymmetrically distributed in the cell membrane. The events occur additionally in the inner mitochondrial membranes (IM) as well as in the endoplasmic reticulum (ER) membrane (Ghomashchi et al. 2010, Singer et al. 2002, Cao et al. 2008, Yang et al. 2004, Nie et al. 2010).

References

- Ghomashchi F, Naika GS, Bollinger JG, Aloulou A, Lehr M, Leslie CC & Gelb MH (2010). Interfacial kinetic and binding properties of mammalian group IVB phospholipase A2 (cPLA₂beta) and comparison with the other cPLA₂ isoforms. *J Biol Chem*, 285, 36100-11. [🔗](#)
- Singer AG, Ghomashchi F, Le Calvez C, Bollinger J, Bezzine S, Rouault M, ... Gelb MH (2002). Interfacial kinetic and binding properties of the complete set of human and mouse groups I, II, V, X, and XII secreted phospholipases A2. *J Biol Chem*, 277, 48535-49. [🔗](#)
- Cao J, Shan D, Revett T, Li D, Wu L, Liu W, ... Gimeno RE (2008). Molecular identification of a novel mammalian brain isoform of acyl-CoA:lysophospholipid acyltransferase with prominent ethanolamine lysophospholipid acylating activity, LPEAT2. *J Biol Chem*, 283, 19049-57. [🔗](#)
- Yang Y, Cao J & Shi Y (2004). Identification and characterization of a gene encoding human LP-GAT1, an endoplasmic reticulum-associated lysophosphatidylglycerol acyltransferase. *J Biol Chem*, 279, 55866-74. [🔗](#)
- Nie J, Hao X, Chen D, Han X, Chang Z & Shi Y (2010). A novel function of the human CLS1 in phosphatidylglycerol synthesis and remodeling. *Biochim Biophys Acta*, 1801, 438-45. [🔗](#)

Edit history

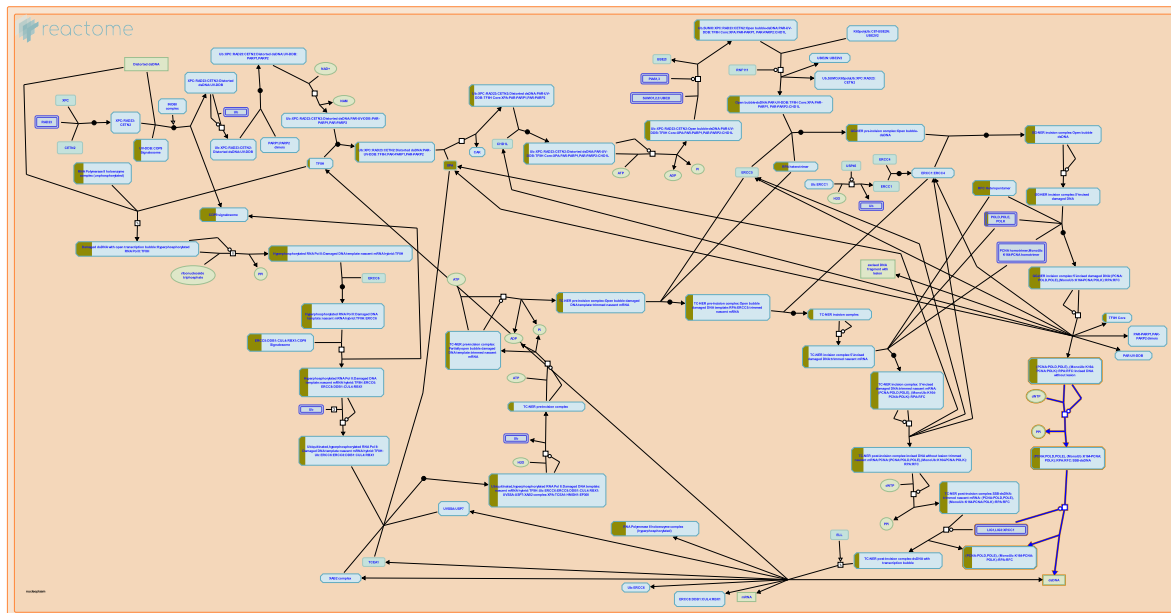
Date	Action	Author
2011-08-12	Edited	Williams MG
2011-08-12	Created	Williams MG

Date	Action	Author
2011-09-14	Authored	Williams MG
2025-11-15	Modified	Weiser JD

4 submitted entities found in this pathway, mapping to 4 Reactome entities

Input	UniProt Id	Input	UniProt Id
CASP6	Q9BZM1	LPGAT1	Q92604
PLA2G3	Q9NZ20	PLA2G4A	P47712

16. Gap-filling DNA repair synthesis and ligation in GG-NER (R-HSA-5696397)



Cellular compartments: nucleoplasm.

Global genome nucleotide excision repair (GG-NER) is completed by DNA repair synthesis that fills the single stranded gap created after dual incision of the damaged DNA strand and excision of the ~27-30 bases long oligonucleotide that contains the lesion. DNA synthesis is performed by DNA polymerases epsilon or delta, or the Y family DNA polymerase kappa (POLK), which are loaded to the repair site after 5' incision (Staresincic et al. 2009, Ogi et al. 2010). DNA ligases LIG1 or LIG3 ligate the newly synthesized stretch of oligonucleotides to the incised DNA strand (Arakawa et al. 2012, Paul-Konietzko et al. 2015).

References

- Staresincic L, Fagbemi AF, Enzlin JH, Gourdin AM, Wijgers N, Dunand-Sauthier I, ... Schärer OD (2009). Coordination of dual incision and repair synthesis in human nucleotide excision repair. *EMBO J.*, 28, 1111-20. [🔗](#)
- Ogi T, Limsirichaikul S, Overmeer RM, Volker M, Takenaka K, Cloney R, ... Lehmann AR (2010). Three DNA polymerases, recruited by different mechanisms, carry out NER repair synthesis in human cells. *Mol. Cell*, 37, 714-27. [🔗](#)
- Arakawa H, Bednar T, Wang M, Paul K, Mladenov E, Bencsik-Theilen AA & Iliakis G (2012). Functional redundancy between DNA ligases I and III in DNA replication in vertebrate cells. *Nucleic Acids Res*, 40, 2599-610. [🔗](#)
- Paul-Konietzko K, Thomale J, Arakawa H & Iliakis G (2015). DNA Ligases I and III Support Nucleotide Excision Repair in DT40 Cells with Similar Efficiency. *Photochem Photobiol*, 91, 1173-80. [🔗](#)

Edit history

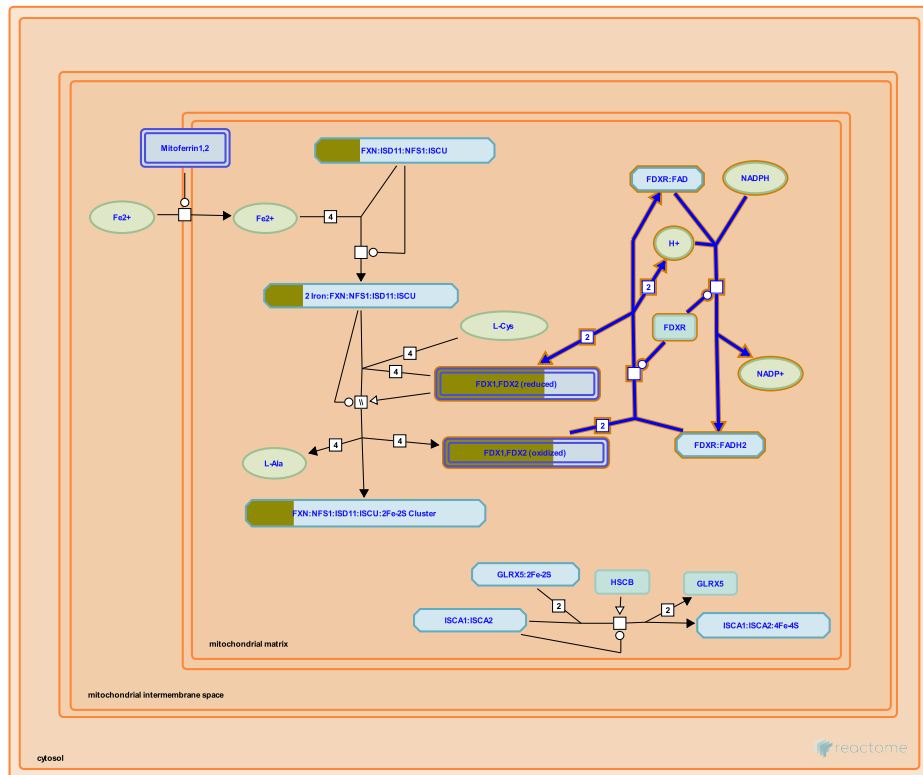
Date	Action	Author
2004-01-29	Authored	Hoeijmakers JH
2004-02-02	Authored	Gopinathrao G
2015-05-28	Created	Orlic-Milacic M

Date	Action	Author
2015-06-16	Revised	Orlic-Milacic M
2015-06-16	Edited	Orlic-Milacic M
2015-06-16	Authored	Orlic-Milacic M
2015-08-03	Reviewed	Fousteri M
2024-02-22	Edited	Orlic-Milacic M

3 submitted entities found in this pathway, mapping to 4 Reactome entities

Input	UniProt Id	Input	UniProt Id	Input	UniProt Id
POLK	Q9UBT6	RFC4	P35249, P35250	RPA3	P35244

17. Electron transport from NADPH to Ferredoxin (R-HSA-2395516)



Cellular compartments: mitochondrial matrix.

NADPH, ferredoxin reductase (FDXR, Adrenodoxin reductase), and ferredoxins (FDX1, FDX1L) comprise a short electron transport chain that provides electrons for biosynthesis of iron-sulfur clusters and steroid hormones (Sheftel et al. 2010, Shi et al. 2012, reviewed in Grinberg et al. 2000, Lambeth et al. 1982).

References

- Shi Y, Ghosh M, Kovtunovych G, Crooks DR & Rouault TA (2012). Both human ferredoxins 1 and 2 and ferredoxin reductase are important for iron-sulfur cluster biogenesis. *Biochim. Biophys. Acta*, 1823, 484-92. [🔗](#)
- Sheftel AD, Stehling O, Pierik AJ, Elsässer HP, Mühlenhoff U, Webert H, ... Lill R (2010). Humans possess two mitochondrial ferredoxins, Fdx1 and Fdx2, with distinct roles in steroidogenesis, heme, and Fe/S cluster biosynthesis. *Proc. Natl. Acad. Sci. U.S.A.*, 107, 11775-80. [🔗](#)
- Grinberg AV, Hannemann F, Schiffler B, Müller J, Heinemann U & Bernhardt R (2000). Adrenodoxin: structure, stability, and electron transfer properties. *Proteins*, 40, 590-612. [🔗](#)
- Lambeth JD, Seybert DW, Lancaster JR, Salerno JC & Kamin H (1982). Steroidogenic electron transport in adrenal cortex mitochondria. *Mol. Cell. Biochem.*, 45, 13-31. [🔗](#)

Edit history

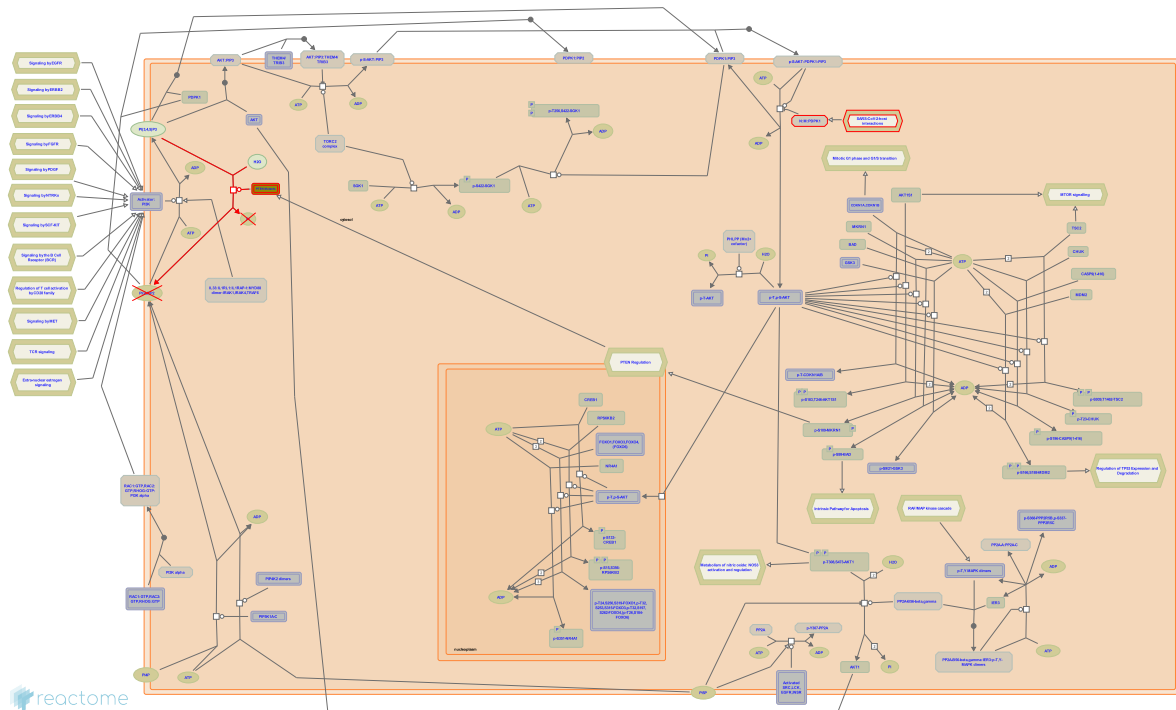
Date	Action	Author
2011-06-04	Authored	May B
2012-06-30	Edited	May B
2012-07-02	Created	May B

Date	Action	Author
2012-09-24	Authored	LiLL R
2012-10-12	Reviewed	Tong WH, Rouault TA
2025-11-15	Modified	Weiser JD

1 submitted entities found in this pathway, mapping to 2 Reactome entities

Input	UniProt Id
FDX1	P10109, Q6P4F2

18. PTEN Loss of Function in Cancer (R-HSA-5674404)



Diseases: cancer.

Loss-of-function mutations affecting the phosphatase domain of PTEN are frequently found in sporadic cancers (Kong et al. 1997, Lee et al. 1999, Han et al. 2000), as well as in PTEN hamartoma tumor syndromes (PHTS) (Marsh et al. 1998). PTEN can also be inactivated by gene deletion or epigenetic silencing, or indirectly by overexpression of microRNAs that target PTEN mRNA (Huse et al. 2009). Cells with deficient PTEN function have increased levels of PIP3, and therefore increased AKT activity. For a recent review, please refer to Hollander et al. 2011.

References

- Kong D, Suzuki A, Zou TT, Sakurada A, Kemp LW, Wakatsuki S, ... Horii A (1997). PTEN1 is frequently mutated in primary endometrial carcinomas. *Nat. Genet.*, 17, 143-4. [🔗](#)
- Lee JO, Yang H, Georgescu MM, Di Cristofano A, Maehama T, Shi Y, ... Pavletich NP (1999). Crystal structure of the PTEN tumor suppressor: implications for its phosphoinositide phosphatase activity and membrane association. *Cell*, 99, 323-34. [🔗](#)
- Han SY, Kato H, Kato S, Suzuki T, Shibata H, Ishii S, ... Ishioka C (2000). Functional evaluation of PTEN missense mutations using in vitro phosphoinositide phosphatase assay. *Cancer Res*, 60, 3147-51. [🔗](#)
- Marsh DJ, Coulon V, Lunetta KL, Rocca-Serra P, Dahia PL, Zheng Z, ... Eng C (1998). Mutation spectrum and genotype-phenotype analyses in Cowden disease and Bannayan-Zonana syndrome, two hamartoma syndromes with germline PTEN mutation. *Hum. Mol. Genet.*, 7, 507-15. [🔗](#)
- Huse JT, Brennan C, Hambardzumyan D, Wee B, Pena J, Rouhanifard SH, ... Holland EC (2009). The PTEN-regulating microRNA miR-26a is amplified in high-grade glioma and facilitates gliomagenesis in vivo. *Genes Dev.*, 23, 1327-37. [🔗](#)

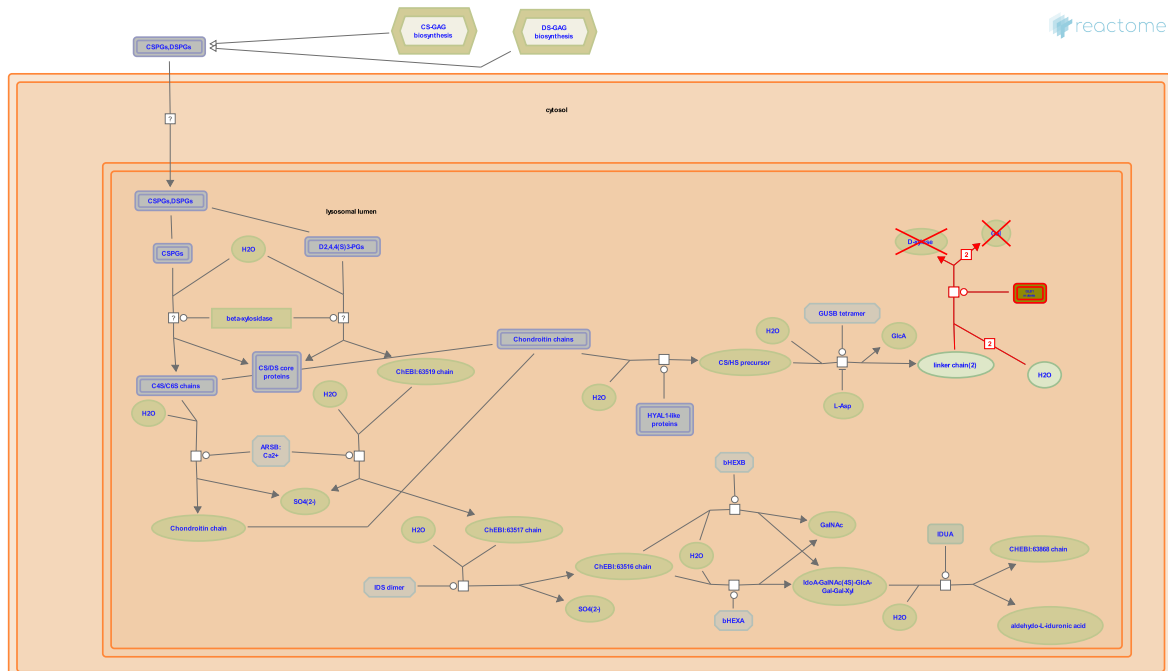
Edit history

Date	Action	Author
2012-07-18	Authored	Orlic-Milacic M
2012-08-13	Reviewed	Yuzugullu H, Thorpe L, Zhao JJ
2015-02-12	Created	Orlic-Milacic M

1 submitted entities found in this pathway, mapping to 1 Reactome entities

Input	UniProt Id
TEP1	P60484

19. MPS IV - Morquio syndrome B (CS/DS degradation) (R-HSA-9953111)



Diseases: mucopolysaccharidosis.

Defects in beta-galactosidase (GLB1; MIM:611458) can result in GM1 gangliosidosis (GM1; MIM:230500) (Nishimoto et al. 1991) (not described here), with several phenotypes indicating mental deterioration, as well as in mucopolysaccharidosis IVB, a characteristic mucopolysaccharidosis with no neurological symptoms (Callahan 1999).

Mucopolysaccharidosis IVB (MPS IVB, Morquio's syndrome B; MIM:253010) is a rare, autosomal recessive mucopolysaccharide storage disease characterized by intracellular accumulation of keratan sulfate (KS), skeletal dysplasia and corneal clouding. There is no central nervous system involvement, intelligence is normal and there is increased KS excretion in urine (Suzuki et al. "Beta-galactosidase deficiency (beta-galactosidosis): GM1 gangliosidosis and Morquio B disease", p3775-3809 in Stryer et al. 2001). MPSIVB is caused by a defect in betagalactosidase (GLB1), which normally cleaves terminal galactosyl residues from glycosaminoglycans, gangliosides and glycoproteins. The GLB1 gene spans 62.5 kb and contains 16 exons (Oshima et al. 1988, Santamaria et al. 2007) and maps to chromosome 3p21.33 (Takano & Yamanouchi 1993).

References

- Nishimoto J, Nanba E, Inui K, Okada S & Suzuki K (1991). GM1-gangliosidosis (genetic beta-galactosidase deficiency): identification of four mutations in different clinical phenotypes among Japanese patients. Am. J. Hum. Genet., 49, 566-74. [\[link\]](#)
- Scriver CR, Beaudet AL, Valle D & Sly WS (2001). *Beta-galactosidase deficiency (beta-galactosidosis): GM1 gangliosidosis and Morquio B disease, The Metabolic and Molecular Bases of Inherited Disease, 8th ed*, 3775-3809.
- Callahan JW (1999). Molecular basis of GM1 gangliosidosis and Morquio disease, type B. Structure-function studies of lysosomal beta-galactosidase and the non-lysosomal beta-galactosidase-like protein. Biochim. Biophys. Acta, 1455, 85-103. [\[link\]](#)

Oshima A, Tsuji A, Nagao Y, Sakuraba H & Suzuki Y (1988). Cloning, sequencing, and expression of cDNA for human beta-galactosidase. *Biochem. Biophys. Res. Commun.*, 157, 238-44. [🔗](#)

Santamaria R, Blanco M, Chabas A, Grinberg D & Vilageliu L (2007). Identification of 14 novel GLB1 mutations, including five deletions, in 19 patients with GM1 gangliosidosis from South America. *Clin. Genet.*, 71, 273-9. [🔗](#)

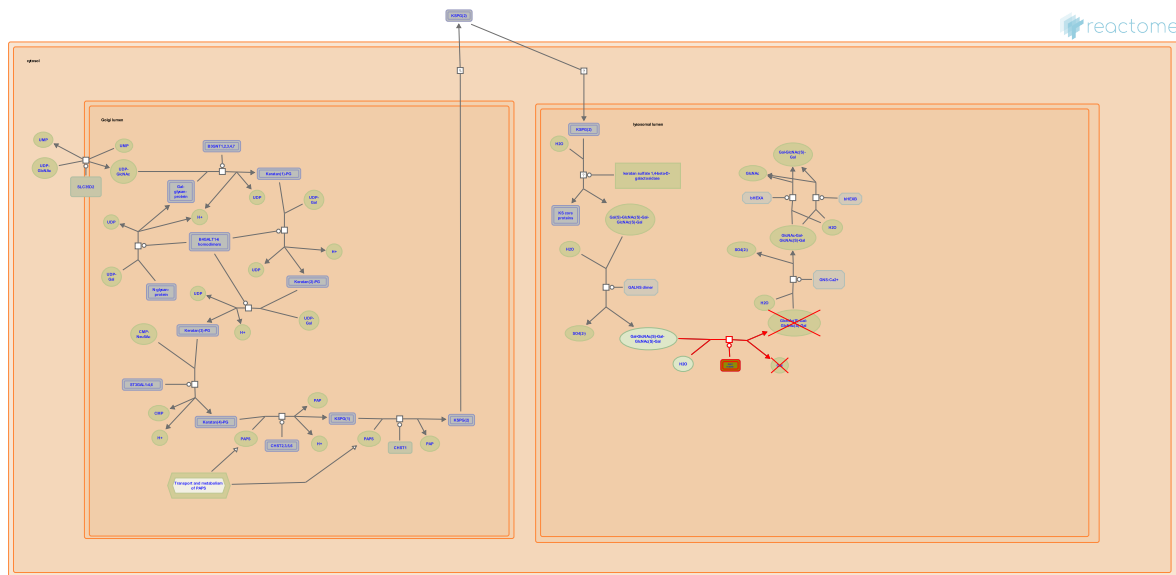
Edit history

Date	Action	Author
2025-05-28	Edited	Stephan R
2025-05-28	Reviewed	Matthews L
2025-05-28	Authored	Stephan R
2025-05-28	Created	Stephan R
2025-05-29	Modified	Stephan R

1 submitted entities found in this pathway, mapping to 1 Reactome entities

Input	UniProt Id
GLB1	P16278

20. MPS IV - Morquio syndrome B (Keratin metabolism) ([R-HSA-2206308](#))



Diseases: mucopolysaccharidosis.

Defects in beta-galactosidase (GLB1; MIM:611458) can result in GM1 gangliosidosis (GM1; MIM:230500) (Nishimoto et al. 1991) (not described here), with several phenotypes indicating mental deterioration, as well as in mucopolysaccharidosis IVB, a characteristic mucopolysaccharidosis with no neurological symptoms (Callahan 1999).

Mucopolysaccharidosis IVB (MPS IVB, Morquio's syndrome B; MIM:253010) is a rare, autosomal recessive mucopolysaccharide storage disease characterized by intracellular accumulation of keratan sulfate (KS), skeletal dysplasia and corneal clouding. There is no central nervous system involvement, intelligence is normal and there is increased KS excretion in urine (Suzuki et al. "Beta-galactosidase deficiency (beta-galactosidosis): GM1 gangliosidosis and Morquio B disease", p3775-3809 in Stryer et al. 2001). MPSIVB is caused by a defect in betagalactosidase (GLB1), which normally cleaves terminal galactosyl residues from glycosaminoglycans, gangliosides and glycoproteins. The GLB1 gene spans 62.5 kb and contains 16 exons (Oshima et al. 1988, Santamaria et al. 2007) and maps to chromosome 3p21.33 (Takano & Yamanouchi 1993).

References

- Nishimoto J, Nanba E, Inui K, Okada S & Suzuki K (1991). GM1-gangliosidosis (genetic beta-galactosidase deficiency): identification of four mutations in different clinical phenotypes among Japanese patients. Am. J. Hum. Genet., 49, 566-74. [\[CrossRef\]](#)

Scriver CR, Beaudet AL, Valle D & Sly WS (2001). *Beta-galactosidase deficiency (beta-galactosidosis): GM1 gangliosidosis and Morquio B disease, The Metabolic and Molecular Bases of Inherited Disease*, 8th ed, 3775-3809.

Callahan JW (1999). Molecular basis of GM1 gangliosidosis and Morquio disease, type B. Structure-function studies of lysosomal beta-galactosidase and the non-lysosomal beta-galactosidase-like protein. Biochim. Biophys. Acta, 1455, 85-103. [\[CrossRef\]](#)

Oshima A, Tsuji A, Nagao Y, Sakuraba H & Suzuki Y (1988). Cloning, sequencing, and expression of cDNA for human beta-galactosidase. Biochem. Biophys. Res. Commun., 157, 238-44. [\[CrossRef\]](#)

Santamaría R, Blanco M, Chabas A, Grinberg D & Vilageliu L (2007). Identification of 14 novel GLB1 mutations, including five deletions, in 19 patients with GM1 gangliosidosis from South America. Clin. Genet., 71, 273-9. [🔗](#)

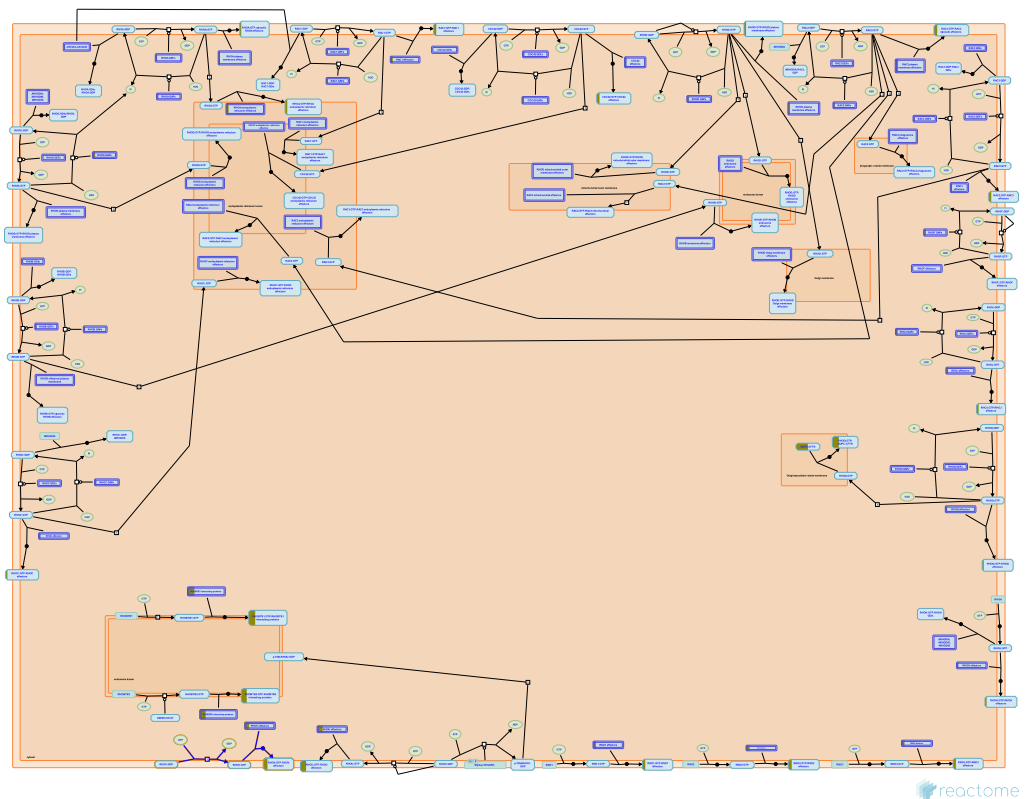
Edit history

Date	Action	Author
2012-04-26	Edited	Jassal B
2012-04-26	Authored	Jassal B
2012-04-26	Created	Jassal B
2012-08-27	Reviewed	Alves S, Coutinho MF
2025-05-28	Modified	Stephan R
2025-05-28	Reviewed	Matthews L

1 submitted entities found in this pathway, mapping to 1 Reactome entities

Input	UniProt Id
GLB1	P16278

21. RHOV GTPase cycle (R-HSA-9013424)



RHOV (also known as Chp) is an atypical RHO GTPase that is thought to be constitutively active due to its high intrinsic guanine nucleotide exchange activity. No guanine nucleotide exchange factors (GEFs) nor GTPase activator proteins (GAPs) that act on RHOV have been identified. RHOV is expressed at very low levels. The expression of RHOV is detected during embryonic development in fish (Tay et al. 2010), frog (Guémar et al. 2007) and chicken (Notarnicola et al. 2008). RHOV is involved in neural crest formation, where its expression is induced downstream of WNT signaling. RHOV is thought to regulate cell adhesion, as its zebrafish orthologue is required for proper localization of E-cadherin and beta-catenin at adherens junctions. RHOV activates JNK and induces apoptosis in rat pheochromocytoma cell line PC12 (Shepelev et al 2011) and in macrophages (Song et al. 2015).

RHOV gene overexpression is a molecular marker of human lung adenocarcinoma (Shepelev and Korobko 2013, Shukla et al. 2017, Ma et al. 2020, Zhang et al. 2020), where RHOV is likely to act as an oncogene (Chen et al. 2021).

For review, please refer to Faure and Fort 2015, and Hodge and Ridley 2020.

References

- Hodge RG & Ridley AJ (2020). Regulation and functions of RhoU and RhoV. *Small GTPases*, 11, 8-15. [🔗](#)
- Faure S & Fort P (2015). Atypical RhoV and RhoU GTPases control development of the neural crest. *Small GTPases*, 6, 174-7. [🔗](#)
- Tay HG, Ng YW & Manser E (2010). A vertebrate-specific Chp-PAK-PIX pathway maintains E-cadherin at adherens junctions during zebrafish epiboly. *PLoS One*, 5, e10125. [🔗](#)

Notarnicola C, Le Guen L, Fort P, Faure S & de Santa Barbara P (2008). Dynamic expression patterns of RhoV/Chp and RhoU/Wrch during chicken embryonic development. Dev Dyn, 237, 1165-71.



Guémar L, de Santa Barbara P, Vignal E, Maurel B, Fort P & Faure S (2007). The small GTPase RhoV is an essential regulator of neural crest induction in Xenopus. Dev Biol, 310, 113-28.



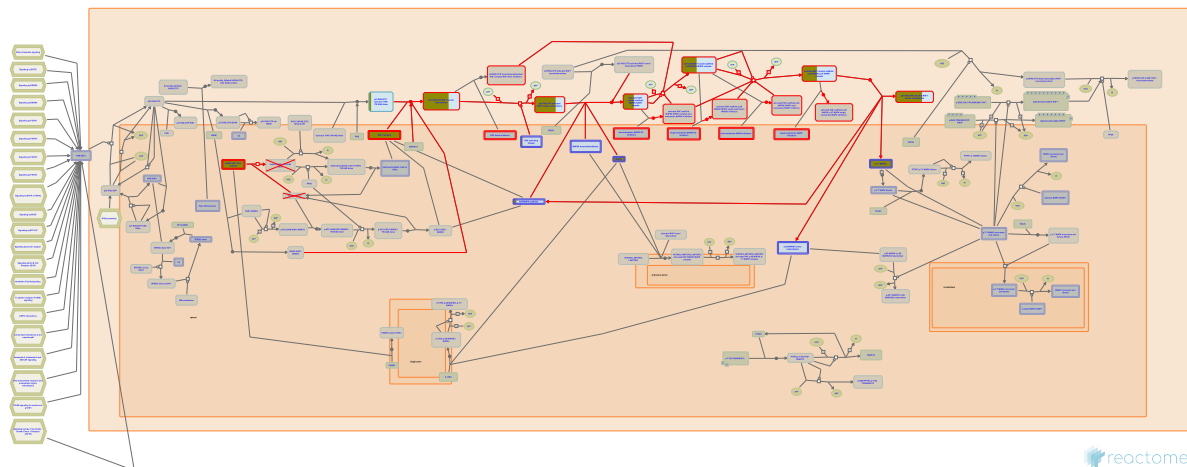
Edit history

Date	Action	Author
2017-07-25	Created	Orlic-Milacic M
2020-07-14	Authored	Orlic-Milacic M
2021-02-05	Reviewed	Fort P
2021-02-25	Edited	Orlic-Milacic M
2021-03-30	Reviewed	Shepelev MV
2021-04-15	Edited	Orlic-Milacic M
2025-11-15	Modified	Weiser JD

5 submitted entities found in this pathway, mapping to 5 Reactome entities

Input	UniProt Id	Input	UniProt Id	Input	UniProt Id
CLNS1A	Q13153	GIT1	Q9Y2X7	PIK3R1	P27986
SPTBN1	Q01082	TXNL1	O43396		

22. Signaling by RAF1 mutants (R-HSA-9656223)



Diseases: Noonan syndrome, cancer, Costello syndrome, LEOPARD syndrome, hypertrophic cardiomyopathy.

RAF1, also known as CRAF, is mutated in a number of germline RASopathies including Noonan Syndrome, Costello Syndrome and others, and also at low frequency in a number of cancers (reviewed in Rauen, 2013; Samatar and Poulikakos, 2015). Activating mutations cluster around conserved region 2 (CR2) which is required for regulation of the protein and the activation segment in CR3 (reviewed in Rauen, 2013).

References

Rauen KA (2013). The RASopathies. *Annu Rev Genomics Hum Genet*, 14, 355-69. [🔗](#)

Samatar AA & Poulikakos PI (2014). Targeting RAS-ERK signalling in cancer: promises and challenges. *Nat Rev Drug Discov*, 13, 928-42. [🔗](#)

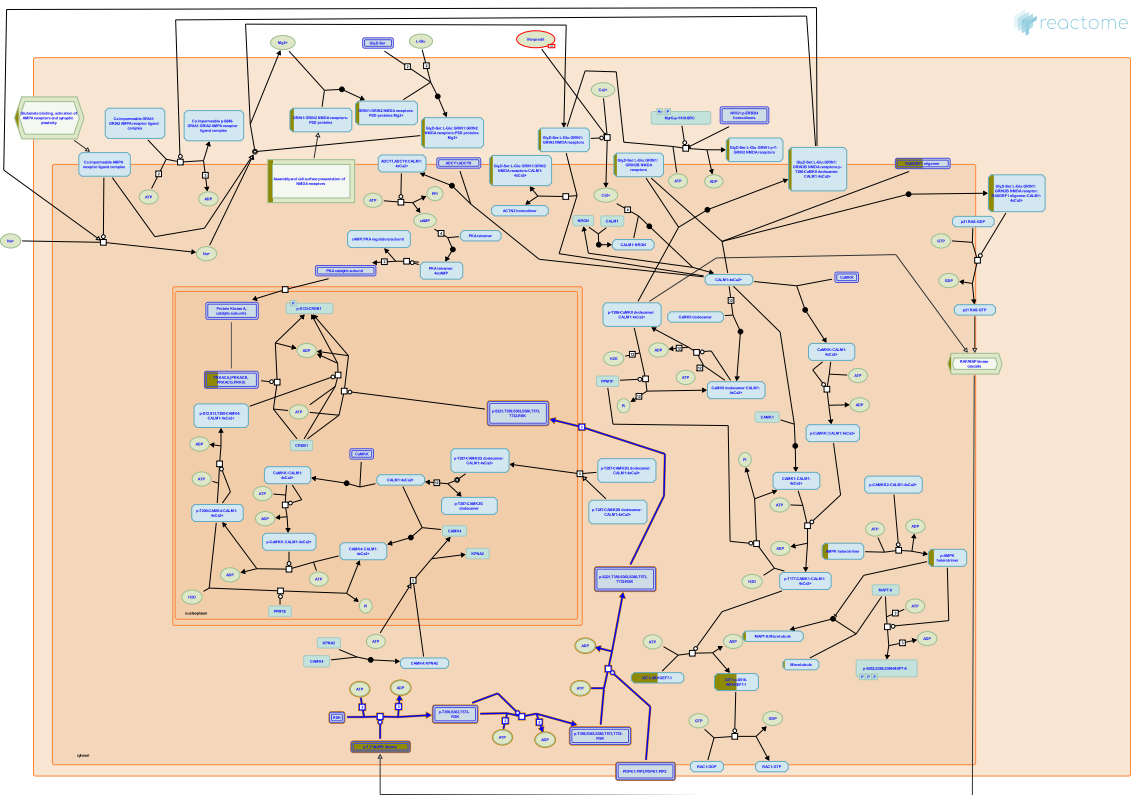
Edit history

Date	Action	Author
2019-07-27	Created	Rothfels K
2019-10-25	Authored	Rothfels K
2020-05-04	Reviewed	Gavathiotis E
2020-05-26	Edited	Rothfels K

5 submitted entities found in this pathway, mapping to 6 Reactome entities

Input	UniProt Id	Input	UniProt Id	Input	UniProt Id
FGA	P02671	MAPK3	P27361, P28482	RAF1	P04049
RAP1A	P62834	VCL	P18206		

23. RSK activation (R-HSA-444257)



Cellular compartments: cytosol, nucleoplasm.

Ribosomal S6 kinase (RSK) has four isoforms in humans, RPS6KA1 (RSK1), RPS6KA2 (RSK3), RPS6KA3 (RSK2) and RPS6KA6 (RSK4), and each of the isoforms have six conserved phosphorylation sites (in RPS6KA1, these are serine residues S221, S363 and S380 and threonine residues T359, T573 and T732). Phosphorylation at four of these residues appears to be critically important for the catalytic activity of RSKs: S221, S363, S380 and T573 (in RPS6KA1).

Phosphorylation and activation of RSKs primarily occurs at the plasma membrane, but can occur in the cytoplasm and in the nucleus. ERKs (MAPK1 and MAPK3), activated downstream of RAS signalling, phosphorylate RSKs on threonine and serine residues T359, S363 and T573 (in RPS6KA1). Phosphorylation by ERKs enables autophosphorylation of RSKs on serine residue S380 and threonine residue T732 (in RPS6KA1). Phosphorylation of RSKs by PDPK1 (PDK1) at serine residue S221 (in RPS6KA1) is necessary for the full activation of RSKs and phosphorylation of RSK substrates (reviewed by Anjum and Blenis 2012). RSK4 differs from other RSKs because it shows high level of constitutive phosphorylation and activity in the absence of growth factors, although it is still responsive to growth factors and ERK activity (Dummller et al. 2005).

RSKs, especially RSK2, are highly expressed in brain regions with high synaptic activity. RSK2 mutations are the underlying cause of Coffin-Lowry syndrome (CLS), which is characterized by cognitive impairment and skeletal anomalies (Zeniou et al. 2002).

References

- Anjum R & Blenis J (2008). The RSK family of kinases: emerging roles in cellular signalling. *Nat Rev Mol Cell Biol*, 9, 747-58. 

Dümmler BA, Hauge C, Silber J, Yntema HG, Kruse LS, Kofoed B, ... Frödin M (2005). Functional characterization of human RSK4, a new 90-kDa ribosomal S6 kinase, reveals constitutive activation in most cell types. *J. Biol. Chem.*, 280, 13304-14. [🔗](#)

Zeniou M, Ding T, Trivier E & Hanauer A (2002). Expression analysis of RSK gene family members: the RSK2 gene, mutated in Coffin-Lowry syndrome, is prominently expressed in brain structures essential for cognitive function and learning. *Hum Mol Genet*, 11, 2929-40. [🔗](#)

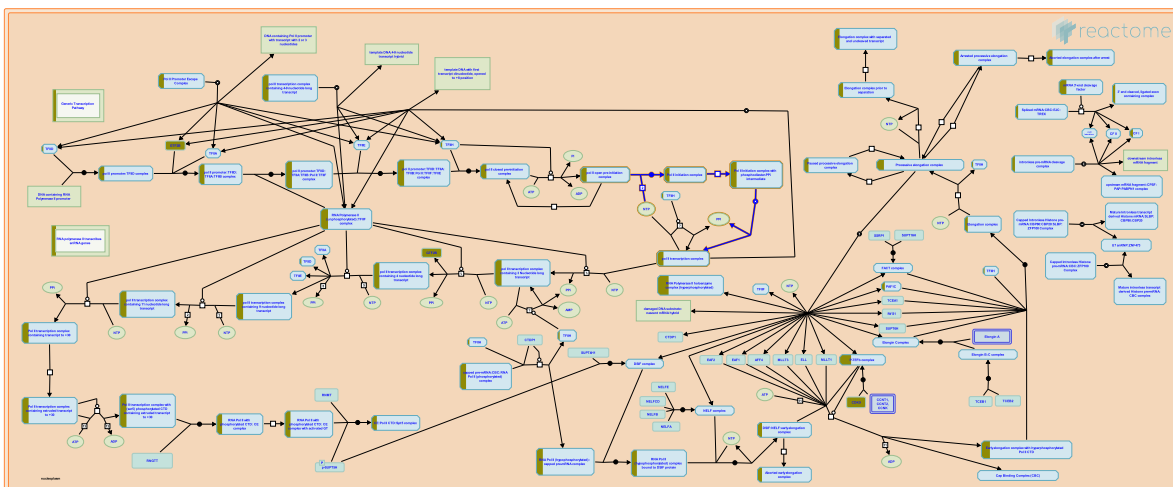
Edit history

Date	Action	Author
2009-10-23	Created	Mahajan SS
2009-10-29	Authored	Mahajan SS
2009-11-18	Reviewed	Tukey D
2009-11-19	Edited	Gillespie ME
2018-10-10	Revised	Orlic-Milacic M
2018-11-02	Reviewed	Hansen KB, Yi F
2018-11-07	Edited	Orlic-Milacic M

1 submitted entities found in this pathway, mapping to 2 Reactome entities

Input	UniProt Id
MAPK3	P27361, P28482

24. RNA Polymerase II Transcription Initiation (R-HSA-75953)



Cellular compartments: nucleoplasm.

Formation of the open complex exposes the template strand to the catalytic center of the RNA polymerase II enzyme. This facilitates formation of the first phosphodiester bond, which marks transcription initiation. As a result of this, the TFIIB basal transcription factor dissociates from the initiation complex.

The open transcription initiation complex is unstable and can revert to the closed state. Initiation at this stage requires continued (d)ATP-hydrolysis by TFIIH. Dinucleotide transcripts are not stably associated with the transcription complex. Upon dissociation they form abortive products. The transcription complex is also sensitive to inhibition by small oligo-nucleotides.

Dinucleotides complementary to position -1 and +1 in the template can also direct first phosphodiester bond formation. This reaction is independent on the basal transcription factors TFIIE and TFIH and does not involve open complex formation. This reaction is sensitive to inhibition by single-stranded oligonucleotides.

References

- Holstege FC, van der Vliet PC & Timmers HT (1996). Opening of an RNA polymerase II promoter occurs in two distinct steps and requires the basal transcription factors IIE and IIH. *EMBO J*, 15, 1666-77. 

Luse DS & Jacob GA (1987). Abortive initiation by RNA polymerase II in vitro at the adenovirus 2 major late promoter. *J Biol Chem*, 262, 14990-7. 

Holstege FC, Fiedler U & Timmers HT (1998). Three transitions in the RNA polymerase II transcription complex during initiation. *EMBO J*, 16, 7468-80. 

Zawel L, Kumar KP & Reinberg D (1995). Recycling of the general transcription factors during RNA polymerase II transcription. *Genes Dev*, 9, 1479-90. 

Kugel JF & Goodrich JA (2002). Translocation after synthesis of a four-nucleotide RNA commits RNA polymerase II to promoter escape. *Mol Cell Biol*, 22, 762-73. 

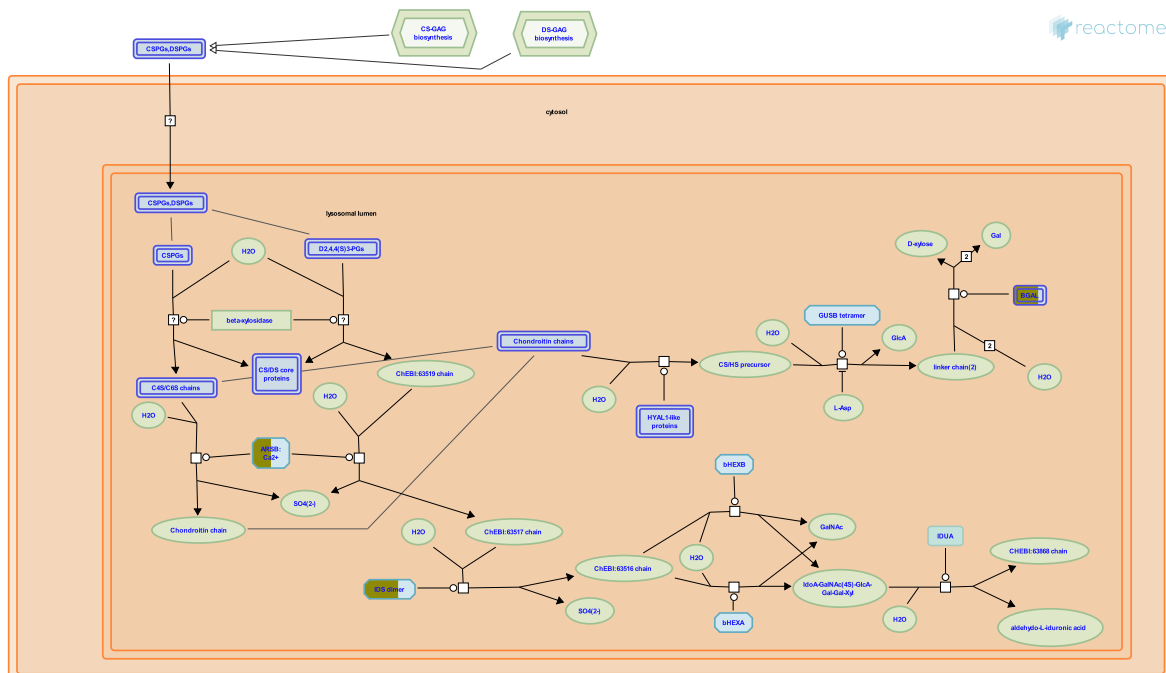
Edit history

Date	Action	Author
2003-09-11	Authored	Timmers HTM
2003-09-11	Created	Timmers HTM
2025-11-12	Edited	Joshi-Tope G
2025-11-15	Modified	Weiser JD

6 submitted entities found in this pathway, mapping to 6 Reactome entities

Input	UniProt Id	Input	UniProt Id	Input	UniProt Id
GTF2B	Q00403	GTF2H2	Q13888	POLR2D	O15514
POLR2J	P52435	TAF11	Q15544	TAF2	Q6P1X5

25. CS/DS degradation (R-HSA-2024101)



Lysosomal degradation of glycoproteins is part of the cellular homeostasis of glycosylation (Winchester 2005). The steps outlined below describe the degradation of chondroitin sulfate and dermatan sulfate. Complete degradation of glycoproteins is required to avoid build up of glycosaminoglycan fragments which can cause lysosomal storage diseases. Complete degradation steps are not shown as they are repetitions of the main ones described here. The proteolysis of the core protein of the glycoprotein is not shown here.

References

Winchester B (2005). Lysosomal metabolism of glycoproteins. *Glycobiology*, 15, 1R-15R. [🔗](#)

Edit history

Date	Action	Author
2011-12-14	Edited	Jassal B
2011-12-14	Authored	Jassal B
2011-12-14	Created	Jassal B
2012-03-28	Reviewed	D'Eustachio P
2025-03-12	Reviewed	D'Eustachio P
2025-05-28	Reviewed	Matthews L
2025-11-15	Modified	Weiser JD

3 submitted entities found in this pathway, mapping to 5 Reactome entities

Input	UniProt Id	Input	UniProt Id	Input	UniProt Id
ARSB	P15848	GLB1	P16278, Q6UWU2, Q8NCI6	IDS	P22304

6. Identifiers found

Below is a list of the input identifiers that have been found or mapped to an equivalent element in Reactome, classified by resource.

593 of the submitted entities were found, mapping to 741 Reactome entities

Input	UniProt Id	Input	UniProt Id	Input	UniProt Id
ABCB6	Q9NP58	ABHD10	Q9NUJ1	ABHD4	Q8TB40
ACAD8	Q9UKU7	ACADL	P28330	ACAN	P16112
ACOT4	Q8N9L9	ACR	P10323	ACSF2	Q96CM8
ADH6	P00325, P28332	ADM2	Q7Z4H4	ADRA2C	P18825
AFMID	Q63HM1	AHI1	Q8N157	AKR7A3	O43488, O95154
ALDH1A3	P47895	ALS2CL	Q60I27	AMELX	Q99217
AMIGO2	Q86SJ2	AMT	P48728	ANGPT1	Q15389
ANK2	Q01484	AOC2	O75106	APBA1	Q02410
APOBEC3G	Q9HC16-1, Q9HC16-3	AQP2	P41181	ARSB	P15848
ATF3	P18847	ATF7IP	Q6VMQ6	ATG101	Q9BSB4
ATG12	O94817	ATG14	Q6ZNE5	ATP12A	P54707
ATP1A1	P05023	ATP2B3	Q16720	ATR	Q13535
AVEN	Q9NQS1	BANF1	O75531	BATF	Q16520
BBIP1	A8MTZ0	BBS5	Q8N3I7	BCL7B	Q9BQE9
BDH2	Q9BUT1	BID	P55957	BIRC2	Q13489, Q13490
BIRC7	Q96CA5	BLTP3B	A0JNW5	BLVRA	P53004
BMP1	P13497	BPIFB1	Q8TDL5	BSN	Q9UPA5
BSND	Q8WZ55	BST2	Q10589	BTK	Q06187
BTN3A1	O00481	BYSL	Q13895	C9orf47	Q99500
CA12	O43570	CA7	P43166	CAMP	P49913
CAPNS1	P04632, Q96L46	CASP6	Q9BZM1	CASQ2	O14958
CATSPER2	Q96P56	CAV2	P51636	CAV3	P56539
CBR1	P16152	CBR4	Q8N4T8	CCDC115	Q96NT0
CCDC12	Q8WUD4	CCDC187	A0A096LP49	CCL2	P13500
CD160	O95971	CD200	P41217	CD53	P19397
CD59	P13987	CDA	P32320	CDC42EP5	Q6NZY7
CDK9	P50750	CDKN1A	P38936	CDKN2C	P42773
CDS2	O95674	CEMIP	Q8WUJ3	CENPN	Q96H22
CER1	O95813	CERS5	Q8N5B7	CES3	P23141
CFP	P27918	CGB3	P0DN86	CHCHD5	Q9BSY4
CHN1	P15882	CHRM5	P08912	CHRNA3	P32297
CHRNA4	P43681	CILP	O75339	CLC	P09496
CLDN11	O75508	CLDN2	P57739	CLNS1A	Q13153
CNTNAP1	P78357	COG7	P83436	COL21A1	Q96P44
COL4A3	Q01955	COLEC11	Q9BWP8	COPS4	Q9BT78
COPS5	Q92905	COPZ1	P61923	COTL1	Q14019
COX11	Q9Y6N1	COX20	Q5RI15	CPSF7	Q8N684
CPT1B	Q92523	CRMP1	Q14194	CSF1R	P07333
CTNNBL1	Q8WYA6	CTRBL1	P17538	CTRC	Q99895
CTSH	P09668	CX3CL1	P78423	CXXC5	Q7LFL8
CYP19A1	P11511	CYP21A2	P08686	CYP2C8	P10632

Input	UniProt Id	Input	UniProt Id	Input	UniProt Id
CYP4B1	P13584	CYP4F2	P78329, Q9HCS2	DAB1	O75553
DAPK1	P53355	DBP	F5HDQ6	DCAF17	Q5H9S7
DDO	Q99489	DDX39B	Q13838	DENND2C	Q68D51
DENND3	A2RUS2	DENND5B	Q6ZUT9	DERL2	Q9GZP9
DGCR8	Q8WYQ5	DHCR7	Q9UBM7	DLG2	Q15700
DLL1	O00548	DNMT3A	Q9Y6K1	DRD1	P21728
DSG1	Q02413	DTX1	Q86Y01	DVL1	O14640
DYNC1LI2	O43237	DYNC2LI1	Q8TCX1	DYNLL1	P63167
DYNLRB1	Q9NP97	EDA2R	Q9HAV5	EDAR	Q9UNE0
EFNA1	P20827	EFNB3	Q15768	EGR1	P18146
EID3	Q8N140	ELOVL2	Q9NXB9, Q9NYP7	ELOVL4	Q9GZR5
ENTPD6	O75354	EPX	P11678	ESD	P10768
ESPNL	Q6ZVH7	ETFBKMT	Q8IXQ9	EVPL	Q92817
EXTL3	O43909	EZH1	Q92800	FABP1	P07148
FANCF	Q9NPI8	FBXL18	Q96ME1	FBXO22	Q8NEZ5
FCGR1BP	Q92637	FDX1	P10109, Q6P4F2	FGA	P02671
FGF2	P09038	FGF7	P21781	FHL2	Q14192
FNTB	P49356	FOLH1	Q04609	FOXO3B	O43524
FRAT2	O75474	FTL	P02792	FXYD6	Q9H0Q3
GALNT4	Q8N4A0	GALR2	O43603	GAS1	P54826
GC	P38435	GCA	P28676	GCLC	P48506
GEMIN4	P57678	GGA3	Q9NZ52	GIT1	Q9Y2X7
GJA9	Q9UKL4	GJB2	P29033	GLB1	P16278, Q6UWU2, Q8NCI6
GLI1	P08151	GLYATL3	Q5SZD4	GMIP	Q9P107
GNAT3	A8MTJ3	GNG8	O14610, Q9UK08	GOPC	Q9HD26
GPAT3	Q53EU6	GPER1	Q99527	GPR18	Q14330
GPR37L1	O60883	GPS1	Q13098	GRK5	P34947
GSTM2	P28161, P46439	GTF2B	Q00403	GTF2H2	Q13888
GUCY1A1	Q02108	GUCY1B2	O75343	H2AC12	Q99878
H2AC15	P0C0S8	H3C13	Q71DI3	H4C16	P62805
HACD1	B0YJ81, Q6Y1H2	HAP1	P27695	HBEGF	Q99075
HEBP2	Q9Y5Z4	HES7	Q9BYE0	HLA-DMB	P28068
HM13	Q8TCT9	HMCN1	Q96DU3	HPGD	P15428
HPX	P02790	HRG	P04196	HS3ST3A1	Q9Y663
HTRA1	Q92743	HTT	P31645	ICAM5	Q9UMF0
ID4	P47928	IDS	P22304	IFIT3	O14879, P09914
IFNL2	Q8IZI9, Q8IZJ0	IGF2	P01344	IGFALS	Q9HBX8
IGHA1	P01876	IGHM	P01871, P01880	IGLL1	P01834
IL11	P20809	IL12RB2	Q99665	IL27	Q8NEV9
ILK	Q13418	IMP4	Q96G21	INHBC	P55103
INMT	O95050	IRF1	P10914	ISL1	P61371
ITGA2	P17301	ITGAD	P20702	JADE1	Q6IE81
JOSD1	Q15040	KCNA6	P17658	KCNH7	Q9NS40
KCNU1	A8MYU2	KDM8	Q8N371	KLHL13	Q9P2J3, Q9P2N7
KLHL21	Q9UJP4	KLK12	Q9UKR0	KMT2B	Q9UMN6
KRTDAP	P60985	LAG3	P18627	LAMTOR5	O43504
LCP2	Q13094	LDHD	Q86WU2	LEO1	Q8WVC0
LGR6	Q9HBX8	LHFPL2	Q6ZUX7	LHFPL5	Q8TAF8
LHX9	Q9NQ69	LIN37	Q96GY3	LMBRD1	Q9NUN5

Input	UniProt Id	Input	UniProt Id	Input	UniProt Id
LPGAT1	Q92604	LRRC8B	Q6P9F7	LRRTM1	Q86UE6
LRRTM2	O43300	LRRTM3	Q86VH5	LSM8	O95777
LTBP1	Q14766	LTf	P02788	LTN1	O94822
LY6E	Q16553	MAFF	Q9ULX9	MALSU1	Q96EH3
MAMLD1	Q13495	MAP3K8	P41279	MAPK11	Q15759
MAPK3	P27361, P28482	MAX	P61244	MC5R	P33032
MCUB	Q9NWR8	MED7	O43513	MEPE	Q9NQ76
MESP1	Q9BRJ9	METTL1	Q9UBP6	MGAT1	P26572
MGAT5B	Q3V5L5	MKLN1	Q9UL63	MMP12	P39900
MMS19	Q96T76	MOGAT1	Q96PD6	MPO	P05164
MRPL20	Q9BYC9	MRPL27	Q8IXM3, Q9P0M9	MRPL9	Q9BYD2
MRPS7	Q9Y2R9	MSRA	Q9UJ68	MTHFD1L	Q6UB35
MTPAP	Q9NNV4	MVB12B	Q9H7P6	MYB	P10242
MYH3	P11055	NAPSA	O96009	NAT8	Q9UHE5
NCKIPSD	Q9NZQ3	NCOA2	Q15596	NDOR1	Q9UHB4
NDST1	P52848	NDUFA4	O00483	NDUFB11	Q9NX14
NDUFB2	O95178	NDUFS6	O75380	NECTIN2	Q92692
NEGR1	Q7Z3B1	NET1	P23975	NFS1	Q9Y697-1
NHS	Q6T4R5	NICN1	Q9BSH3	NLGN2	Q8NFZ4
NLGN4Y	Q8NFZ3	NLRP12	P59046	NOD2	Q9HC29
NOXO1	Q8NFA2	NPC2	P61916	NPR1	P16066
NR4A2	P43354	NSDHL	Q15738	NSF	P46459
NT5C1B	Q9BXI3	NTSR2	O95665	NUP37	Q8NFH4
NXF2	Q9GZY0	OBP2B	P31025	OCLN	Q16625
ODAD3	Q3MIN7	OGDH	Q02218	OPRK1	P41145
OR11H7	Q8NGC8	OR1F1	O43749	OR1L8	Q8NGR8
OR51B4	Q9Y5P0	OR51E1	Q8TCB6	ORM2	P19652
OTUD3	Q5T2D3	OTULIN	Q96BN8	OXCT1	P55809, Q9BYC2
P2RX1	P51575	P2RX7	Q99572	P2RY11	Q96G91
PCBP4	P57723	PCDH19	Q8TAB3	PCSK6	P29122
PDCD7	Q8N8D1	PDE6D	O43924	PDGFRA	P16234
PEMT	Q9UBM1	PEX13	Q92968	PFDN4	Q9NQP4
PGLYRP1	O75594	PGM2L1	Q6PCE3	PGS1	Q32NB8
PHF2	O75151	PHIP	Q8WWQ0	PHYH	O14832
PIGF	Q07326	PIGN	O95427	PIGR	P01833
PIGS	Q96S52	PIGU	Q9H490	PIK3R1	P27986
PIWIL2	Q8TC59	PIWIL4	Q7Z3Z4	PKNOX1	P55347
PLA2G3	Q9NZ20	PLA2G4A	P47712	PLPPR3	Q6T4P5
PLXNA1	Q9UIW2	PLXNC1	O60486	POLK	Q9UBT6
POLR1D	P0DPB5	POLR2D	O15514	POLR2J	P52435
PPARD	Q03181	PPP3CB	P48454	PPP6C	O00743
PPWD1	Q96BP3	PRDM14	Q9GZV8	PRDM7	Q9NQW5
PRICKLE1	Q96MT3	PRKAA1	Q13131	PRKRIP1	Q9H875
PRKX	P51817	PROKR1	Q8TCW9	PRR5	P85299
PRSS3	P35030	PSMB3	P49720	PSMD12	O00232
PSMD13	Q9UNM6	PSMG3	Q9BT73	PTCH2	Q9Y6C5
PTGER3	P43115	PTGER4	P35408	PTH1R	Q03431
PTPN2	P17706	PTPRJ	Q12913	PTPRS	Q13332
PURA	P30520	PYGM	P11217	QSOX1	O00391

Input	UniProt Id	Input	UniProt Id	Input	UniProt Id
RAB17	Q9H0T7	RAB5IF	Q9BUV8	RAD51D	O75771
RAF1	P04049	RANGAP1	P46060	RANGRF	Q9HD47
RAP1A	P62834	RAP1GDS1	P52306	RAPGEF4	Q8WZA2
RASAL1	O95294	RASGRF2	O14827	RB1CC1	Q8TDY2
RBL2	Q08999	RBM23	Q14498	REL	Q00653
RFC4	P35249, P35250	RGL1	Q9NZL6	RGS20	O76081
RGS6	P49758	RHPN1	Q8TCX5	RIGI	O95786
RIMS1	Q86UR5	RNF121	O95998	RNPC3	Q96LT9
RPA3	P35244	RPL10L	Q96L21	RPL17	P18621
RPL24	P83731	RPL30	P62888	RRAGB	Q5VZM2
RSAD2	Q8WXG1	RWDD2B	Q9Y3V2	S100A10	P60903
SALL4	Q9UJQ4	SAMHD1	Q9Y3Z3	SBF2	Q86WG5
SEC24D	O94855	SECISBP2	Q96T21	SEPSECS	Q9HD40
SETDB1	Q15047	SF1	Q13285	SHH	Q15465
SIGLEC10	A6NMB1	SIRPA	P78324	SIX2	Q9NPC8
SKP1	P63208	SLC11A1	P49279	SLC12A4	Q9UP95
SLC18A3	Q16572	SLC24A3	Q9HC58	SLC24A4	Q8NFF2
SLC25A4	P12235	SLC25A42	Q86VD7	SLC37A2	Q8TED4-2
SLC38A3	Q99624	SLC41A2	Q96JW4	SLC51A	Q86UW1
SLC5A4	Q9NY91	SLC7A10	Q9NS82	SLC7A2	P52569-1, P52569-2
SLC7A9	P82251	SLITRK6	Q9H5Y7	SOCS1	O15524
SOCS5	O75159	SP100	P23497	SPINT2	O43291
SPTBN1	Q01082	SPTLC3	Q9NUV7	SRD5A1	P18405
SRSF5	Q13243	ST3GAL5	Q9UNP4	ST8SIA1	Q92185
ST8SIA2	Q92186	STAM	Q75886, Q92783	STARD10	Q9Y365
STC2	O76061	STING1	Q86WV6	STK3	Q13188
SYCE1	Q8N0S2	SYCP3	Q8IZU3	SYNGR1	O43759
SYT2	Q8N9I0	SYT4	Q9BT88	TAF11	Q15544
TAF2	Q6P1X5	TARS1	P26639	TAX1BP1	Q86VP1
TDO2	P48775	TDP2	O95551	TEC	Q92570-1, Q92570-2
TEP1	P60484	TGFBI	P01137	TIMM10B	Q9Y5J6
TLL1	O43897	TMEM11	P17152	TMEM115	Q12893
TMOD1	P28289	TNFAIP8L3	Q5GJ75	TNFRSF12A	Q9NP84
TNFRSF17	Q02223	TNFRSF21	O75509	TNFSF10	P50591
TNPO1	Q92973	TRAPPC10	P48553	TRAPPC6B	O75865, Q86SZ2
TRIM10	Q9UDY6	TRIM62	Q9BVG3	TRIM69	Q86WT6
TRIP11	Q15643	TRMT61B	Q9BVS5	TRPA1	O75762
TRPM6	Q9BX84	TRPV5	Q9NQA5	TSEN54	Q7Z6J9
TSNAX	Q99598	TTLL12	Q14166	TTLL5	Q6EMB2
TTLL8	A6PVC2	TUBB8	Q3ZCM7	TULP4	Q9NRJ4
TXNL1	O43396	TXNRD2	Q9NNW7	UBA5	Q9GZZ9
UBE2A	P49459	UBE2J2	Q8N2K1-1	UBXN11	Q5T124
UCN2	Q96RP3	UGT2B15	P54855	UNC5D	Q6UXZ4
UQCC6	Q69YU5	USH1G	Q495M9	USP2	O75604
USP30	Q70CQ3	UTP25	Q68CQ4	UTP6	Q9NYH9
VBP1	P61758	VCL	P18206	VPS29	Q9UBQ0
VTN	P04004	WARS1	P23381	WAS	P42768
WBP4	O75554	WDR81	Q562E7	WDR83	Q9BRX9
WDTC1	Q8N5D0	WNT11	O96014	WRAP53	Q9BUR4

Input	UniProt Id	Input	UniProt Id	Input	UniProt Id
XPA	P23025	ZDHHC21	Q8IVQ6	ZMAT2	Q96NC0
ZNF138	P52744	ZNF16	Q7L2R6	ZNF175	Q9Y473
ZNF205	O95201	ZNF214	Q9UL59	ZNF215	Q8NE65, Q9UL58
ZNF224	Q9NZL3	ZNF266	Q14584	ZNF268	Q96BR6
ZNF311	Q5JNZ3	ZNF317	Q96PQ6	ZNF354B	Q96LW1
ZNF37A	P17032	ZNF383	Q8NA42, Q8NDQ6, Q9BR84	ZNF398	Q9BS31
ZNF431	Q8TF32	ZNF433	Q8N7K0	ZNF471	Q9BX82
ZNF486	Q96H40	ZNF510	Q9Y2H8	ZNF567	Q8N184
ZNF621	Q6ZSS3	ZNF709	Q8N972	ZNF846	P17019

Input	Ensembl Id	Input	Ensembl Id	Input	Ensembl Id
ALDH1A3	ENST00000329841	ATF3	ENSG00000162772	ATR	ENSG00000175054, ENST00000350721
BATF	ENSG00000156127	BID	ENSG00000015475	BIRC7	ENSG00000101197
BST2	ENSG00000130303	CASP6	ENSG00000138794	CCL2	ENSG00000108691
CDKN1A	ENSG00000124762, ENST00000244741	CER1	ENST00000380911	CGB3	ENSG00000104827
CSF1R	ENSG00000182578	CTRB1	ENST00000361017	CTRC	ENST00000375949
CXXC5	ENSG00000171604	DBP	ENSG00000105516	DHCR7	ENSG00000172893
DLL1	ENSG00000198719	EGR1	ENSG00000120738	ELOVL2	ENSG0000012660
EXTL3	ENSG00000012232	FABP1	ENSG00000163586	FGF2	ENSG00000138685
FHL2	ENSG00000115641	FTL	ENST00000331825	GCLC	ENSG0000001084
GLI1	ENSG00000111087	HES7	ENSG00000179111	ID4	ENSG00000172201
IFIT3	ENSG00000119917	IGF2	ENST00000337883, ENST00000381406	IL12RB2	ENSG00000081985
IRF1	ENSG00000125347	ISL1	ENSG00000016082	ITGA2	ENSG00000164171
MESP1	ENSG00000166823	MYB	ENSG00000118513	OCLN	ENSG00000197822
OPRK1	ENSG00000082556	OR11H7	ENSG00000258806	OR1F1	ENSG00000168124
OR1L8	ENSG00000171496	OR51B4	ENSG00000183251	OR51E1	ENSG00000180785
PCBP4	ENSG00000090097	PCDH19	ENSG00000165194	PIK3R1	ENSG00000145675
POLR2D	ENST00000272645	PRSS3	ENST00000379405	PTCH2	ENSG00000117425
PTPN2	ENSG00000175354	RAD51D	ENSG00000185379, ENST00000345365	RBL2	ENSG00000103479
RGL1	ENSG00000143344	RNU12	ENST00000362512	RNU5A-1	ENSG00000199568
RSAD2	ENSG00000134321	SALL4	ENSG00000101115	SAMHD1	ENSG00000101347
SHH	ENSG00000164690	SIX2	ENSG00000170577	SOCS1	ENSG00000185338
SP100	ENSG00000067066	TEC	ENSG00000119508	TEP1	ENSG00000171862
TGFB1	ENSG00000105329	TNFRSF21	ENSG00000146072	TRIM10	ENSG00000204613
TRIM62	ENSG00000116525	WNT11	ENSG00000085741		

Interactors (658)

Input	UniProt Id	Interacts with	Input	UniProt Id	Interacts with
ABHD10	Q9NUJ1	Q5T4S7	ABHD4	Q8TB40	Q6ZPD8
ACADL	P28330	P22735	ACAN	P16112	P05067
ACSF2	Q96CM8	Q6ZPD8	ACTMAP	Q5BKX5-3	Q9NQ94
ACTR6	Q9GZN1	O95619	ADRA2C	P18825	O14964
AGFG2	O95081	Q9NQZ5	AHI1	Q8N157	P50570
AKAP11	Q9UKA4	P51530	AKR1C8	Q5T2L2	P55212
AKR7A3	O95154	P13569	ANGPT1	Q15389	Q02763, Q15389

Input	UniProt Id	Interacts with	Input	UniProt Id	Interacts with
ANK2	Q01484	Q9P2E9	ANKRD45	Q5TZF3-1	Q96CV9
ANKS6	Q68DC2	P01031	APBA1	Q02410	O14936
APOBEC3G	Q9HC16	P69723	AQP2	P41181	P24593
ARMC7	Q9H6L4	Q96RU7	ARRDC4	Q8NCT1	Q96J02
ARSB	P15848	P01185	ATF3	P18847	P18848
ATF7IP	Q6VMQ6	Q15047	ATG101	Q9BSB4	O75385
ATG12	O94817	Q9H1Y0, Q9H0Y0, Q9NT62, Q676U5	ATG14	Q6ZNE5	P41208
ATP1A1	P05023	P12931	ATPAF1	Q5TC12	P06576
ATR	Q13535	Q9NZQ7	BANF1	O75531	O75531
BATF	Q16520	P18848	BAZ1A	Q9NRL2	O60264
BBIP1	A8MTZ0	Q96RK4, Q8N3I7	BBS5	Q8N3I7	A8MTZ0, Q8IWZ6, Q96RK4, Q3SYG4, Q8NFJ9, Q8TAM2, Q9BCX9
BCL7B	Q9BQE9	Q969G3, Q12824	BCLAF1	Q9NYF8	P10415
BEX5	Q5H9J7	O14561	BID	P70444, P55957, P70444- PRO_0000223236	Q07812
BIRC2	Q13490	Q9NP84, P36941	BIRC7	Q96CA5	P49638
BLOC1S2	Q6QNY1	A1L4H1	BLTP3B	A0JNW5	P31946
BLVRA	P53004	Q9H244	BMP1	P13497	O60216
BPIFB1	Q8TDL5	Q16822	BSND	Q8WZ55	Q05329
BST2	Q10589	Q10589	BTK	Q06187	Q06187
BTN3A1	O00481-2, O00481	O60437	BYSL	Q13895	O14641
C10orf88	Q9H8K7	Q13163	C11orf68	Q9H3H3	Q15056
C19orf38	A8MVS5	Q16625	C7orf25	Q9BPX7	P49792
C9orf47	Q99500	P21964	CALCOCO1	Q9P1Z2	O14965
CALR3	Q96L12	Q8WXG9	CAMP	Q96JM3	Q9UI95
CAPNS1	P04632	P01375	CARHSP1	Q9Y2V2	Q13077
CASP6	P55212	Q8WUX9	CASQ2	O14958	P62736
CATIP	Q7Z7H3	Q9H8M2	CAV2	P51636	Q15392
CAV3	P56539	P0DOE7	CBLC	Q9ULV8	Q9BQP7
CBR1	P16152	O75828	CC2D1A	Q6P1N0	Q9H444
CCDC102A	Q96A19	O15392	CCDC112	Q8NEF3-2	Q9Y2T1
CCDC115	Q96NT0	O15342	CCDC12	Q8WUD4	Q16629
CCDC127	Q96BQ5	P41208	CCDC158	Q5M9N0-2	P07550
CCDC70	Q6NSX1	P01375	CCDC71L	Q8N9Z2	Q9Y4Z2
CCL2	P13500	P13501	CCM2L	Q9NUG4	Q9NZ43
CD160	O95971	Q92956	CD200	P41217	Q8TD46
CD53	P19397	P78382	CD59	P13987	Q15363
CDA	P32320	Q96QG7	CDK9	P50750	Q9HAW4
CDKN1A	P38936	Q99741	CDKN2C	P42773	P01185
CDPF1	Q6NVV7	O43559	CDR2	Q01850	P51530
CDS2	O75420	Q86UK7	CELSR2	Q9HCU4	Q92838
CENPN	Q96H22	Q13352	CENPV	Q7Z7K6	Q92993
CER1	O95813	P35813	CERS5	Q8N5B7	Q9H244
CFAP52	Q8N1V2	P31948	CFP	P27918	Q6Y288
CGB3	P0DN86	P01215	CHCHD5	Q9BSY4	P53701
CHN1	P15882	P28482	CHRM5	P08912	P20309
CHRNA3	P32297	Q8NC56	CHRNA4	P43681	P17302

Input	UniProt Id	Interacts with	Input	UniProt Id	Interacts with
CIART	Q8N365	O75553	CIB4	A0PJX0	Q99757
CLC	Q9UBD9, Q9UBD9-PRO_0000015616	P26992, O75462	CLDN11	O75508	P26715
CLDN2	P57739	Q96CW1	CLNS1A	P54105	P18509
CLSTN1	O94985	Q01523	CLSTN3	Q8IUW6	P02649
CNTNAP1	P78357	Q9H2A9	COBL	O75128	P13196
COBLL1	Q53SF7	P31946	COG7	P83436	Q9NZQ7
COLEC11	Q9BWP8-PRO_0000315044	P07911	COPS4	Q9BT78	P61081
COPS5	Q92905	P19838	CORO1B	Q9BR76	Q9NWB7
COTL1	Q14019	P09917	COX11	Q9Y6N1	Q9Y337
COX20	Q5RI15	Q9BZP6	CPSF7	Q8N684-3, Q8N684	O43809
CPT1B	A2RRE8	P42858	CRB1	P82279	Q8N3R9
CREBZF	Q9NS37	P18848	CRIPPT	Q9P021	P78352
CRMP1	Q14194	O15169	CRYGS	P22914	Q9P032
CSF1R	P09581, P07333	P09603	CSTPP1	Q9H6J7-2	P02649
CT45A10	P0DMU9	O00560	CTAG2	O75638	Q0VG06
CTDSP1	Q9GZU7	Q9NW38	CTNNBL1	Q8WYA6	Q9UKN5
CTRC	Q99895	Q8NBK3	CTSH	P09668	P07711
CX3CL1	P78423	P05556	CYP21A2	Q08AG9	Q12837
CYP4F2	P78329	Q96QE2	DAB1	O75553-5, O75553	Q13526
DAPK1	P53355	P14618-1	DBP	Q10586	P35638
DDX39B	Q13838	Q09161	DENND2C	Q68D51-2	P07947
DERL2	Q9GZP9	Q9NR28	DGCR8	Q8WYQ5	P46087
DHCR7	Q9UBM7	P13569	DKK3	Q9UBP4	P12236
DKKL1	Q9UK85	O75197	DLG2	Q15700	O60469
DLX3	O60479	Q12837	DNMT3A	Q9Y6K1	Q9Y6K1
DPCD	Q9BVM2	Q92696	DRD1	P21728	Q13324-2
DSG1	Q02413	P13569	DTX1	Q86Y01	Q96J02
DVL1	O14640	P49674	DYNC1LI2	O43237	P13569
DYNC2LI1	Q8TCX1	P00441	DYNLL1	P63167	Q6W0C5
DYNLRB1	Q9NP97	P10636-8	DYRK4	Q9NR20	Q92630
EDA2R	Q9HAV5	Q13114	EDAR	Q9UNE0	Q92838
EDRF1	Q3B7T1	O14832	EFNA1	P20827	P54764
EFNB3	Q15768	P54764	EGR1	P18146	Q8N726
EID3	Q8N140	Q9H4I9	EIF6	P56537	P19525
ELOVL2	Q9NYP7	P09601	ELOVL4	Q9GZR5	Q07817
ENOX1	Q8TC92	O00560	ENTPD6	O75354	P27824
ERMAP	Q96PL5	Q86VM9	ESPNL	Q6ZVH7	Q5SW96
ETFBKMT	Q8IXQ9	P10809	EVPL	Q92817	Q9Y324
EXTL3	O43909	Q9H8X2	EZH1	Q92800	P15056
FABP1	P07148	P54764	FAM110B	Q8TC76	P49674
FAM111B	Q6SJ93	Q01105	FAM172A	Q8WUF8	P63208
FAM184A	Q8NB25	P06396	FAM204A	Q9H8W3	O60341
FAM222A	Q5U5X8	Q9UBE8	FAM234B	A2RU67	O43913
FANCD2OS	Q96PS1	Q5W0B1	FANCF	Q9NPI8	O15360, O15287
FBXL18	Q96D16	P61978	FBXO22	Q8NEZ5	O14867
FBXO24	O75426	P08238	FBXO3	Q9UK99	P04608
FBXO46	Q6PJ61	Q92905	FGA	P02671	P02647
FGF2	P09038	P21802	FHL2	Q14192	Q9UBZ9

Input	UniProt Id	Interacts with	Input	UniProt Id	Interacts with
FIBP	O43427	P80370	FMC1	Q96HJ9	Q9NUJ1
FNDC3A	Q9Y2H6	O43511	FNTB	P49356	P01185
FOXRED2	Q8IWF2	Q9UBV2	FRAT2	O75474	P49841
FTL	P02792	Q8WVC6	FXYD6	Q9H0Q3	Q9UBD6
GALNT4	Q8N4A0	Q13790	GATAD1	Q8WUU5	Q13547
GC	P38435	P0DTC5	GCA	P28676	Q13077
GCLC	P48506	Q6IPR3	GEMIN4	P57678	Q13304
GGA3	Q9NZ52	Q6VY07	GIT1	Q9Y2X7	Q99728
GJB2	P29033	P29033, P08034	GKAP1	Q5VSY0	Q92993
GLB1	P16278	P61586	GLI1	P08151	Q9UMX1, Q96J02
GLIPR1L2	Q4G1C9	Q6VN20	GNG8	Q9UK08	P49959
GOLGA6L9	A6NEM1	Q13415	GOLGA8G	Q08AF8	Q00994
GOPC	Q9HD26	Q6UWP7	GPAT3	Q53EU6	Q9H2J7
GPATCH2L	Q9NWQ4-1	Q96RU7	GPR155	Q7Z3F1	P25090
GPR160	Q9UJ42	P17252	GPR18	Q14330	P42357
GPR37L1	O60883	Q14162	GPS1	Q13098	Q9BYZ6, Q94844
GRAMD2B	Q96HH9	Q12981	GRK5	P34947	P25963
GTF2B	Q00403	P30740	GTF2H2	Q13888	P50613
GTF2H2C	Q6P1K8	P50613	H2AC15	P0C0S8	O95760
H3C13	Q71DI3	P62805	H4C16	P62805	P0DTC4
HACD1	B0YJ81	P46059	HAP1	P54257	A6NI15
HBEGF	Q99075	P00533	HDHD5	Q9BXW7	P10809
HELZ	P42694	Q8IWL3	HES7	Q9BYE0	P47897
HM13	Q8TCT9	P04578	HOXA5	P20719	Q96RT1
HOXA9	EBI-1801917	Q03164	HOXD13	P35453	P00740
HRG	P04196	Q96PM5	HSPB6	O14558	P46821
HTRA1	Q92743	P78504	HTT	P42858	Q9UP65
ICAM5	Q9UMF0	Q8WY64	ID4	P47928	Q9Y4Z2
IDS	P22304	Q8NBK3, Q8NBJ7	IFIT3	O14879	Q92905
IFNL2	Q8IZJ0	Q8IU54	IGF2	P01344	P24593, P22692
IGHA1	P01876	Q00403	IGHM	P01871	Q99856
IL12RB2	Q99665	Q14765	ILK	Q13418	P04049
IMP4	Q8TCT7-2	Q00403	IRF1	P15314	Q13114
ISL1	P61371	Q9Y4X5	ISY1-RAB43	Q9ULR0-1	O43559
ITGA2	P17301	Q9H0F6	ITM2A	O43736	P05067-4
JADE1	Q6IE81-3	Q96CV9	JOSD1	Q15040	P22735
KCNA6	P17658	Q9UPQ8	KCTD12	Q96CX2	Q9UJK0
KDM8	Q8N371	A6NED2	KLF6	Q99612	Q04206
KLHL13	Q9P2N7	P01282	KLHL17	Q6TDP4	P07585
KLHL21	Q9UJP4	P23025	KMT2B	Q9UMN6	O00255
LAMTOR5	O43504	P68104	LAPTM4A	Q15012	P14927
LCP2	Q13094	P19174	LDAF1	Q96B96	Q05329
LEO1	Q8WVC0	P23193	LGALS8	O00214	Q7Z2H8
LHFPL2	Q6ZUX7	Q14162	LHFPL5	Q8TAF8	P78382
LHX6	Q9UPM6	O14832	LHX9	Q9NQ69	P68400
LIN37	Q96GY3	P10243	LPGAT1	Q92604	P22732
LPP	Q93052	P05120	LRFN5	Q96NI6	P23468, Q13332
LRRC36	Q1X8D7	Q9UMX1	LRRC73	Q5JTD7	Q6UWV6
LRRC8B	Q6P9F7	Q13370	LRRN1	O75427	A1L3X0

Input	UniProt Id	Interacts with	Input	UniProt Id	Interacts with
LRRTM1	Q86UE6	Q13370	LRRTM2	O43300	P01375
LRRTM3	Q86VH5	O95470	LRWD1	Q9UFC0	Q9Y5N6
LSM8	O95777	P62306, P14678	LTBP1	Q14766	P06276
LTF	P02788	Q9HA64	LTN1	O94822	Q9Y5B0
LXN	Q9BS40	Q9UQK1	MACIR	Q96GV9	O00410
MAFF	Q9ULX9	O14867	MAGEA12	P43365	P01160
MAGEA4	P43358	Q9NUX5	MAGEC3	Q8TD91-2	P78333
MAL2	Q969L2	P49638	MALSU1	Q96EH3	Q14197
MAP3K2	Q9Y2U5	Q13163	MAP3K8	P41279	P19838, Q8NFZ5
MAPK11	Q15759	P49137	MAPK3	P27361	P19419
MAX	P61244	P04198	MCUB	Q9NWR8	Q15047
MEA1	Q16626	Q96CW1	MED7	O43513	Q15648
MEGF8	Q7Z7M0	P22692	MEPE	Q9NQ76	P98164
METTL17	Q9H7H0	Q9UBX5	MGAT1	P26572	Q9BYC5
MICALL2	Q8IY33	P12814	MKLN1	Q9UL63	Q13685
MKRN2	Q9H000	P51668	MMS19	Q96T76	P51530
MOB3C	Q70IA8	Q9NRD5	MORC3	Q14149	Q9NWF9
MPO	P05164	P27797	MRPL20	Q9BYC9	P40429
MRPL27	Q9P0M9, Q8IXM3	Q14197	MRPL9	Q9BYD2	P21673
MRPS7	Q9Y2R9	P67809	MTHFD1L	Q6UB35	Q96GW9
MTPAP	Q9NVV4	Q9UHD2	MYADM	Q96S97	P43115
MYB	P10242	P63165, P61956	MYH3	P11055	Q15475
MYPOP	Q86VE0	P21673	NAA16	Q6N069-4	P14136
NAP1L5	Q96NT1	P18848	NAPSA	O96009	P11021
NAT8	Q9UHE5	Q9H2K0	NCKIPSD	Q9NZQ3	Q9UQB8
NCOA2	Q15596	O00482-1	NDOR1	Q9UHB4	Q9UBE8
NDST1	P52848	Q03405	NDUFA4	O00483	Q9UI09
NDUFB11	Q9NX14	P08034	NDUFB2	Q9Y6T4	O00311
NDUFS6	O75380	P25103	NEBL	O76041	Q9Y6D9
NECTIN2	Q92692-2	P07237	NEGR1	Q7Z3B1	P61916
NET1	Q7Z628	Q14160	NEURL4	Q96JN8	Q9UJU6
NFXL1	Q6ZN86	Q96FT7	NHS	Q6T4R5	O43639
NHSL1	Q5SYE7	P16333	NICN1	Q9BSH3	P0CG47
NLGN2	Q8NFZ4	Q8N0Z6	NLRP12	P59046	P08631
NOD2	Q9HC29	P29466	NPC2	P61916	P00751
NR4A2	P43354	P05067	NSF	P46459	P59635
NUP37	Q8NFH4	Q8WYP5	NXF2	Q9GZY0	Q9BYW2
NXPE1	Q8N323	P12830	OCLN	Q16625	P18827
OCM	P0CE72	O00560	ODAD3	A5D8V7	Q96LB3, Q9H7X7, Q8WYA0
OGDH	Q02218	P13569	OGDHL	Q9ULD0	P11802
OLFML2A	Q68BL7	Q15848	OPRK1	P41145	P35414
ORM2	Q06144	Q96BA8	OTULIN	Q96BN8	Q12981
OXCT1	P55809	P42566	P2RX1	P51575	O95470
P2RX7	Q99572	P14373	PABPC3	Q9H361	P67809
PCBP4	P57723	P11142	PCED1B	Q96HM7	Q7Z3S9
PCGF1	Q9BSM1	Q03111	PCNP	Q8WW12	O75533
PCSK6	P29122	P0DTC8	PDCD7	Q8N8D1	Q15696
PDE6D	O43924	P36404	PDGFRA	P16234	P46109
PEMT	P15941-11	Q96AA3	PEX13	Q92968	O00628

Input	UniProt Id	Interacts with	Input	UniProt Id	Interacts with
PFDN4	Q9NQP4	Q13164	PHF2	O75151	Q96RI1
PHRF1	Q9P1Y6	P67870	PHYH	O14832	O75925
PIGF	Q07326	Q8N661	PIGN	O95427	P43119
PIGR	P01833	Q00403	PIGS	Q96S52	Q7Z3S9, P0DPK4
PIH1D1	Q9NWS0	Q7KZ85, Q96JC9	PIK3R1	P27986	O15455
PIMREG	Q9BSJ6	P04156	PIWIL4	Q7Z3Z4	Q9Y2W6
PKDCC	Q504Y2	Q9H5K3	PKNOX1	P55347	P40424
PLEKHB1	Q9UF11	P52306	PLXNA1	Q9UIW2	Q01523, P59665
PLXNC1	O60486	O75326	PM20D2	Q8IYS1	O75695
PNRC1	Q12796	Q9NPI6	POGLUT3	Q7Z4H8	P0DTC8
POLR1D	P0DPB6	O15160, Q9GZS1, O95602, O15446, Q9H9Y6, P19388, P61218, P62875	POLR2D	O15514	O60942, O00267
			PPARD	Q03181-2	P40763
POLR2J	P52435	Q9Y5B0	PPP1R18	Q6NYC8	Q969Y2
PPP1R16B	Q96T49	P40937	PPP3CB	P16298	P14316
PPP1R37	O75864	O75593	PPWD1	Q96BP3	P55735
PPP6C	O00743	O43318	PRDM7	Q9NQW5	Q13077
PRDM14	Q9GZV8	Q8IVS8	PRKAA1	Q13131	O75385
PRICKLE1	Q96MT3	Q9HAQ2	PRKX	P51817	Q13451
PRKRIP1	Q9H875	P62304	PRTFDC1	Q9NRG1	Q8NFF5
PRR5	P85299-2	O14964	PSMD12	O00232	O00487
PSMB3	P49720	O00487	PSMG3	Q9BT73	Q9BQB4
PSMD13	Q9UNM6	O00487	PTH1R	Q03431	P35222
PTGER3	P43115	P27037	PTPRJ	Q62884	P12931
PTPN2	P17706	Q9Y5K5	PURA	Q00577	P19525
PTPRS	Q13332	Q16288	RAB5IF	Q9BUV8	O60704
RAB17	Q9H0T7	P24386	RAD51D	O75771	O43543, O43502, O15315
RABL3	Q5HYI8	Q9NRZ7	RAI2	Q9Y5P3	P07196
RAF1	P04049	P43246	RANGAP1	P46060	P61769
RALGPS2	Q86X27	P31947	RAP1A	P62834	P04049
RANGRF	Q9HD47	Q8N307	RAPGEF4	Q8WZA2	P05455
RAP1GDS1	P52306	P17480	RBL2	Q08999	P11802
RB1CC1	Q8TDY2	O75385	RBM45	Q8IUH3	Q9Y316
RBM23	Q86U06	Q9Y5V3	RCSD1	Q6JBY9	P52907
RBM48	Q5RL73	Q8NFP9	REP15	Q6BDI9	Q99856
REL	Q04864-2	P30622	RFC4	P35249	P35250, P0CG13, P40938, P40937, Q9BVC3, Q8WVB6
REX1BD	Q96EN9	O00487			
RGS20	O76081-6	Q8WUK0	RGS6	P49758	P08238
RHPN1	Q8TCX5	Q9NZ53	RIGI	O95786	P59596
RIMS1	Q86UR5	P06241	RIPPLY1	Q0D2K3	Q13114
RNASEH2A	O75792	Q99943	RNF166	Q96A37	P36941
RNPC3	Q96LT9	Q15696	RPA3	P35244	P23025
RPL10L	Q96L21	Q99558	RPL17	P18621	P63244
RPL24	P83731	Q99558	RPL30	P62888	Q15361
RPRM	Q9NS64	O60493	RRAGB	Q5VZM2-2, Q5VZM2	Q9Y2Q5, Q0VGL1, Q6IAA8, O43504, Q8NBW4, Q9UHA4
RSAD2	Q8WXG1	P55056, P02654	RWDD2B	P57060	Q96HC4
S100A10	P60903	P03950	SAMHD1	Q9Y3Z3	P20248

Input	UniProt Id	Interacts with	Input	UniProt Id	Interacts with
SASS6	Q6UVJ0	Q9HC77	SBF2	Q86WG5	Q13614
SCGN	O76038	Q12846	SCML1	Q9UN30-2	O00560
SCYL3	Q8IZE3, Q8IZE3-2	Q99757	SEC24D	O94855, O94855-2	Q15436
SECISBP2	Q96T21	Q08379	SEPSECS	Q9HD40	P04591
SETDB1	Q15047-2	O94844	SEZ6L2	Q6UXD5	P17931
SF1	Q13285	P61024	SGTB	Q96EQ0	P01229
SHC4	Q6S5L8	P00533	SHH	Q62226, Q15465	Q4KMG0, Q96QV1
SHROOM1	Q2M3G4	P54652	SIRPA	P78324	Q08722
SIX2	Q9NPC8	Q7Z5W3	SKAP1	Q86WV1	O15117
SKP1	P63208	P38936	SLC12A4	Q9UP95	P17931
SLC16A6	O15403	O76024	SLC24A3	Q9HC58	Q86TM6
SLC25A4	P12235	P12236	SLC25A48	Q6ZT89	Q13077
SLC35A5	Q9BS91	Q9NTJ5	SLC35F1	Q5T1Q4	P21964
SLC41A2	Q96JW4	Q9H2J7	SLC41A3	Q96GZ6	Q86UT5
SLC51A	Q86UW1	P0CG47	SLC7A2	P52569	P30825
SLMAP	Q14BN4	Q9BRV8	SMOC1	Q9H4F8	Q04721
SMR3A	Q99954	O00308	SNX24	Q9Y343, Q9Y343-2	P49674
SOCS1	O15524	P46109	SOCS5	O75159	Q93034, Q9UBF6
SP100	P23497	Q9Y6K1	SP140	Q13342	Q13526
SPINT2	O43291	Q5K4L6	SPTBN1	Q01082	P62993
SRPX	P78539	Q9BRX2	SRSF5	Q13243	Q9NYV4, Q14004
ST8SIA1	Q92185	Q96CV9	STAM	Q92783	O95630
STARD10	Q9Y365	Q96LA8	STC2	O76061	P0DTC8
STING1	Q86WV6	Q96N66	STK3	Q13188	P18509
STMN3	Q9NZ72	Q16512	STRIP2	Q9ULQ0	Q9BRV8
SYCE1	Q8N0S2	P09917	SYCP3	Q8IZU3	P51587
SYNDIG1	Q9H7V2	Q9H1C4	SYNGR1	O43759-2	P29274
SYNPO	Q8N3V7	P04156	SYT2	Q8N9I0	P98155
SYT4	Q9H2B2	Q14596	SYTL3	Q4VX76	P51159
TACSTD2	P09758	Q9UNU6	TAF2	Q6P1X5	P35249
TAMALIN	Q7Z6J2	Q9BYF1	TARS1	P26639	Q96CV9
TAX1BP1	Q86VP1	O15111	TBC1D5	Q92609	Q9BZP6
TCEAL5	Q5H9L2	P43354	TDO2	P48775	P12830
TDP2	O95551	O14641	TEC	Q92570	Q9H2F3
TEFM	Q96QE5	O00411	TENT5B	Q96A09	O95947
TEP1	P60484	Q8NI35	TEX29	Q8N6K0	Q02094
TGFB1	P01137	O60551	THYN1	Q9P016	Q9UHJ6
TIGD3	Q6B0B8	Q92466	TIMM10B	Q9Y5J6	P18509
TM2D1	Q9BX74	P05067	TM9SF4	Q92544	P13726
TMEM102	Q8N9M5	Q96QF0	TMEM11	P17152	Q16585
TMEM115	Q12893	Q86U10	TMEM164	Q5U3C3	Q9H244
TMEM171	Q8WVE6	O43913	TMEM176A	Q96HP8	Q9H2K0
TMEM38A	Q9H6F2	O60496	TMOD1	P28289	P06396
TMTc4	Q5T4D3	Q9Y4Z2	TNFAIP8L3	Q5GJ75	O00560
TNFRSF12A	Q9NP84	Q9BRI3	TNFRSF17	Q02223	Q9Y5Y5
TNFRSF21	O75509	P08138	TNFSF10	P50591	O15519-2, O15519-1
TNPO1	Q92973	P52272	TRAPPC10	P48553	Q9P2M4
TRAPPC6B	Q86SZ2	Q9P2M4	TRIM10	Q9UDY6	Q9UHD2
TRIM23	P36406	Q8NFF5	TRIM62	Q9BVG3	P51668
TRIM69	Q86WT6, Q86WT6-2	P08243	TRIP11	Q15643	P31946

Input	UniProt Id	Interacts with	Input	UniProt Id	Interacts with
TRIP13	Q15645	Q8NDV7	TRMT61B	Q9BVS5	Q4G176
TRPV5	Q9NQA5	Q96T88	TSEN54	Q7Z6J9	Q92989
TSNAX	Q99598	Q00994	TSPAN3	O60637	Q9NPF0
TTC23L	Q6PF05	A6NI15	TTLL12	Q14166	P68104
TUBB8	Q3ZCM7	Q96JA1	TULP4	Q9NRJ4	Q93034, Q9UBF6
TUSC1	Q2TAM9	O95749	TXNL1	O43396	P10636-8
UBA5	Q9GZZ9	Q15067	UBE2A	P49459	Q8WZA2
UBE2J2	Q8N2K1	A1L3X0	UBXN11	Q5T124	O94955
UBXN2B	Q14CS0	Q02548	UPRT	Q96BW1	Q9NWZ5
USH1G	Q495M9	Q9UER7	USP2	O75604-3	Q00403
USP30	Q70CQ3	Q9H5K3	USP35	A2RRA6	O76024
UTP25	Q68CQ4	P32121	UTP6	Q9NYH9	P32455
VBP1	P61758	Q13164	VCL	P18206, P18206-2	P35221
VPS29	Q9UBQ0	O60493	VPS8	Q8N3P4	P21462
VSIG1	Q86XK7	O43808	VTN	P04004	P05121
VWA5B2	Q8N398	P20336	WARS1	P23381	P13569
WAS	P42768	Q05209	WBP4	O75554	P62306
WDFY4	Q6ZS81-2	Q96CV9	WDR55	Q9H6Y2	P06748
WDR62	O43379	P45983	WDR81	Q562E7	Q14508
WDR83	Q9BRX9	O75695	WDTC1	Q8N5D0	Q13371
WRAP53	Q9BUR4	O60832, Q9NY12, Q9NPE3	XPA	P23025	Q99856
YPEL2	Q96QA6	Q9NRD5	ZBTB2	Q8N680	P07237
ZC2HC1B	Q5TFG8	O43639	ZC3H10	Q96K80	O75593
ZCCHC10	Q8TBK6	O94782	ZDHHC21	Q8IVQ6	Q16581
ZER1	Q7Z7L7	Q6IN84	ZMAT2	Q96NC0	Q9NUJ1
ZMYND12	Q9H0C1	Q9UI95	ZNF138	P52744	Q96EB6
ZNF175	Q9Y473	P13196	ZNF205	O95201	Q9NRD5
ZNF214	Q9UL59	Q9NS56	ZNF224	Q9NZL3	P98164
ZNF266	Q14584	Q9HD47	ZNF268	Q14587	O15431
ZNF292	O60281	P83916	ZNF317	Q96PQ6	P98175
ZNF384	EBI-11743072	P14373	ZNF398	Q8TD17	Q96CV9
ZNF431	Q8TF32	P17643	ZNF471	Q9BX82	Q8N9N5
ZNF511	Q8NB15	Q9UI95	ZNF567	Q8N184	Q13263
ZNF57	Q68EA5	Q9NPB3	ZNF621	Q6ZSS3	P45973
ZNF836	Q6ZNA1	P05067	ZRANB2	O95218	P32121, P49407
Input	ChEBI Id	Interacts with	Input	ChEBI Id	Interacts with
BMP1	P13497	29108	IL11	P20809	29108
NPC2	P61916	16113	TLL1	O43897	29108

7. Identifiers not found

These 889 identifiers were not found neither mapped to any entity in Reactome.

A2M-AS1	ABHD8	ACBD3-AS1	ACBD7-DCLRE1CP1	ACTR3-AS1	ADAM20P1	ADCY10P1	ADM-DT
ADM5	AFAP1L2	AFF2	AGAP5	AKNA	AMN1	AMZ2P1	ANKDD1A
ANKFN1	ANKRD18CP	ANKRD26P3	ANKRD34C	ANKRD65-AS1	ANP32A-IT1	ANP32C	APOA1-AS
APOBEC3D	APTR	AQP5-AS1	AQP7P3	ARHGAP44-AS1	ARL17B	ARLNC1	ASAP1-IT2
ATP5MGL	ATRIP-TREX1	BARX1	BCAN-AS1	BCLAF3	BMAL2-AS1	BOK-AS1	BVES-AS1
C11orf58	C11orf97	C12orf54	C17orf100	C18orf61	C1QTNF8	C1orf56	C20orf203
C2orf81	C4orf46P3	C5orf34-AS1	C6orf132	CASTOR3P	CC2D2B	CCDC110	CCDC126
CCDC175	CCDC3	CCDC88C-DT	CCL8	CCNT2-AS1	CCNYL2	CCSER1	CDKN2A-DT
CDRT15	CDRT15P1	CECR2	CENPBD2P	CEP128	CFAP54	CHEK2P2	CHROMR
CIROP	CLIP1-AS1	CLYBL-AS3	CNBD1	CNTN4-AS1	COL4A2-AS1	COMMD5P1	COX7B2
CPQ	CRYBG2	CSTF3-DT	CT47B1	CTDP1-DT	CYP21A1P	CYYR1	DDX43
DEFB131B	DENN6A-DT	DHRS12	DIRC3	DLEU7-AS1	DLG5-AS1	DNAJB3	DNMT3L-AS1
DPH5-DT	DUSP28	EFR3A	EGFLAM	EGFR-AS1	EIF2AK3-DT	EPHA1-AS1	EPIC1
ERICH6B	ERVH48-1	ESPNP	EVX1	EWSAT1	FAM153B	FAM169A-AS1	FAM186B
FAM200A	FAM224A	FAM230I	FAM30C	FAM88F	FAM95A	FAR2P2	FBXW4P1
FGF7P3	FHIP1A	FKBP1A-SDCBP2	FLICR	FLJ20021	FLJ30679	FLVCR2	FNDC1
FNDC10	FOSL2-AS1	FRG1JP	FSTL4	GAGE10	GAL3ST2	GDPD4	GGTL2
GHET1	GIMAP8	GLTPD2	GOLGA6L1	GOLGA6L25	GOLGA6L26	GOLGA8EP	GPATCH3
GPR153	GPR63	GRTP1	GTF2IP4	GTF3C2-AS1	GUSBP11	GUSBP15	GUSBP17
Gene	H3P4	H3P6	HDAC2-AS2	HES2	HLA-DQB1-AS1	HMGN4	HMGXB3
HOMER3-AS1	HOXA-AS3	HOXA10-HOXA9	HOXC6	HP09053	HSDL2-AS1	HSPA12A-AS1	HTR7P1
IGFL2	IGHVIII-38-1	IGIP	IGSF1	IGSF21	IKZF2	IMPG2	INKA2
INVS	IQCM	IRX4-AS1	ISM2	KAAG1	KCNIP2-AS1	KIF5C-AS1	KIZ-AS1
KLRA1P	LAMTOR5-AS1	LEF1-AS1	LENEP	LIM2	LINC00032	LINC00115	LINC00278
LINC00501	LINC00578	LINC00640	LINC00663	LINC00664	LINC00696	LINC00847	LINC00885
LINC01090	LINC01166	LINC01168	LINC01179	LINC01278	LINC01340	LINC01341	LINC01366
LINC01372	LINC01416	LINC01467	LINC01516	LINC01555	LINC01569	LINC01664	LINC01694
LINC01822	LINC02014	LINC02102	LINC02117	LINC02228	LINC02256	LINC02294	LINC02321
LINC02348	LINC02371	LINC02381	LINC02394	LINC02428	LINC02507	LINC02637	LINC02688
LINC02718	LINC02739	LINC02764	LINC02797	LINC02851	LINC02883	LINC02918	LINC02926
LINC02975	LINC02984	LINC03000	LINC03060	LIPE-AS1	LL0XNC01-250H12.3	LMLN-AS1	LNCPRESS1
LNCTAM34A	LOC100130587	LOC100130744	LOC100131496	LOC100288123	LOC100505909	LOC100506023	LOC100506235
	LOC100506532	LOC100506606	LOC100507387	LOC100507403	LOC100652777	LOC100996598	LOC100996842
	LOC101927245	LOC101927259	LOC101927272	LOC101927383	LOC101927452	LOC101927550	LOC101927608
	LOC101928119	LOC101928191	LOC101928215	LOC101928217	LOC101928347	LOC101928438	LOC101928502
	LOC101929200	LOC101929230	LOC101929298	LOC101929314	LOC101929452	LOC101929633	LOC101929692
	LOC101929719	LOC101930048	LOC102723313	LOC102723334	LOC102723340	LOC102723345	LOC102723370
	LOC102723534	LOC102723575	LOC102723670	LOC102723675	LOC102723758	LOC102724046	LOC102724151
	LOC102724351	LOC102724410	LOC102724687	LOC102724723	LOC103171574	LOC105369183	LOC105369228
	LOC105369406	LOC105369534	LOC105369587	LOC105369745	LOC105369781	LOC105369811	LOC105369823
	LOC105369999	LOC105370090	LOC105370148	LOC105370274	LOC105370322	LOC105370337	LOC105370406
	LOC105370421						

LOC105370519	LOC105370534	LOC105370601	LOC105370679	LOC105370787	LOC105370790	LOC105370926	LOC105371036
LOC105371098	LOC105371103	LOC105371227	LOC105371235	LOC105371277	LOC105371345	LOC105371499	LOC105371502
LOC105371516	LOC105371554	LOC105371559	LOC105371597	LOC105371600	LOC105371675	LOC105371701	LOC105371709
LOC105371722	LOC105371755	LOC105371793	LOC105371855	LOC105371864	LOC105371942	LOC105371951	LOC105371956
LOC105372016	LOC105372088	LOC105372253	LOC105372266	LOC105372348	LOC105372356	LOC105372410	LOC105372451
LOC105372506	LOC105372507	LOC105372513	LOC105372553	LOC105372594	LOC105372617	LOC105372666	LOC105372668
LOC105372671	LOC105372815	LOC105372816	LOC105372839	LOC105372841	LOC105372902	LOC105373024	LOC105373138
LOC105373190	LOC105373302	LOC105373346	LOC105373447	LOC105373475	LOC105373583	LOC105373623	LOC105373652
LOC105373673	LOC105373793	LOC105373811	LOC105373871	LOC105373883	LOC105373992	LOC105373994	LOC105374069
LOC105374103	LOC105374171	LOC105374298	LOC105374314	LOC105374329	LOC105374344	LOC105374347	LOC105374418
LOC105374795	LOC105374800	LOC105374811	LOC105374928	LOC105374938	LOC105374945	LOC105374986	LOC105375221
LOC105375536	LOC105375647	LOC105375719	LOC105375771	LOC105375779	LOC105375884	LOC105375913	LOC105376037
LOC105376042	LOC105376093	LOC105376126	LOC105376127	LOC105376159	LOC105376216	LOC105376231	LOC105376235
LOC105376270	LOC105376299	LOC105376447	LOC105376486	LOC105376533	LOC105376724	LOC105376730	LOC105376754
LOC105376825	LOC105376839	LOC105376938	LOC105376950	LOC105376958	LOC105377091	LOC105377212	LOC105377345
LOC105377473	LOC105377527	LOC105377645	LOC105377862	LOC105377905	LOC105378008	LOC105378052	LOC105378148
LOC105378274	LOC105378408	LOC105378452	LOC105378456	LOC105378609	LOC105378632	LOC105378650	LOC105378675
LOC105378768	LOC105378780	LOC105378808	LOC105378944	LOC105378973	LOC105379039	LOC105379047	LOC105379066
LOC105379325	LOC105379364	LOC105379377	LOC105379443	LOC105379490	LOC107983969	LOC107984023	LOC107984035
LOC107984037	LOC107984109	LOC107984126	LOC107984131	LOC107984210	LOC107984264	LOC107984268	LOC107984285
LOC107984298	LOC107984301	LOC107984316	LOC107984340	LOC107984468	LOC107984469	LOC107984494	LOC107984654
LOC107984670	LOC107984776	LOC107984803	LOC107984852	LOC107984906	LOC107985152	LOC107985154	LOC107985181
LOC107985188	LOC107985216	LOC107985263	LOC107985282	LOC107985297	LOC107985303	LOC107985314	LOC107985323
LOC107985345	LOC107985359	LOC107985360	LOC107985393	LOC107985400	LOC107985416	LOC107985438	LOC107985502
LOC107985508	LOC107985551	LOC107985567	LOC107985568	LOC107985570	LOC107985664	LOC107985687	LOC107985698
LOC107985733	LOC107985782	LOC107985783	LOC107986174	LOC107986211	LOC107986373	LOC107986428	LOC107986468
LOC107986477	LOC107986550	LOC107986622	LOC107986714	LOC107986814	LOC107986852	LOC107986853	LOC107986859
LOC107986897	LOC107986909	LOC107986985	LOC107987107	LOC107987147	LOC107987210	LOC107987220	LOC107987233
LOC107987258	LOC107987280	LOC107987364	LOC107987374	LOC112267879	LOC112267930	LOC112267957	LOC112267992
LOC112268049	LOC112268052	LOC112268053	LOC112268056	LOC112268062	LOC112268070	LOC112268076	LOC112268109
LOC112268166	LOC112268196	LOC112268218	LOC112268222	LOC112268235	LOC112268269	LOC112268273	LOC112268276
LOC112268311	LOC112268420	LOC112268426	LOC112268455	LOC158435	LOC286177	LOC339685	LOC389705
LOC440700	LOC440910	LOC644215	LOC644285	LOC653513	LOC728392	LOC90246	LRATD1
LRRC17	LRRC37A6P	LRRC4	LRRC69	LRTM2	LY6-E-DT	LY6G5C	LY75
LYPD9P	MAGOH-DT	MAJIN	MAP4K1-AS1	MARK2P9	MCM3AP-AS1	MCPH1-AS1	MED8-AS1
MFSD13B	MFSD6L	MIG7	MIR10525	MIR10527	MIR12127	MIR1270	MIR1276
MIR1291	MIR202HG	MIR2110	MIR3064	MIR3173	MIR3174	MIR320A	MIR34AHG
MIR3657	MIR3926-2	MIR3940	MIR4469	MIR4507	MIR4639	MIR4641	MIR4664
MIR4672	MIR4685	MIR4700	MIR4721	MIR4751	MIR4758	MIR499B	MIR5088
MIR568	MIR590	MIR600HG	MIR637	MIR6501	MIR6719	MIR6748	MIR6749
MIR6766	MIR6783	MIR6789	MIR6803	MIR6832	MIR6891	MIR7-1	MIR7114
MIR7155	MIR9-1HG	MKRN9P	MMP21	MPP7-DT	MRGPRE	MRGPRG-AS1	MRNIP-DT
MROH7	MRPS30-DT	MRPS9-AS1	MSMB	MSRA-DT	MSTO2P	MTRNR2L9	MYO1H
MYO7B	NDRG3	NDUFB2-AS1	NDUFS2-AS1	NEDD8-MDP1	NETO1-DT	NEUROD2	NEXMIF
NFIA-AS2	NFYC-AS1	NGFR-AS1	NIT1	NLRP14	NPIPBP11	NSMCE1-DT	NUDT16L2P
OCLNP1	OGA	OVOL1-AS1	PAQR5-DT	PARP11-AS1	PAXBP1-AS1	PCAT18	PCDHA9
PCDHGB8P	PCF11-AS1	PDLIM3	PDS5B-DT	PFN4	PIM2	PIP5KL1	PMS2P7
PNCK	PNPLA1	PORCN-DT	POU5F1P3	PPIAL4C	PPP4R1-AS1	PPP4R4	PRAMEF36P
PRIMA1	PRKCZ-DT	PSMD6-AS2	PTCSC2	PTOV1-AS2	PWAR5	PXK	R3HCC1L
RANBP3-DT	RASSF3-DT	RASSF9	RBAKDN	RBPM5-AS1	RDH10-AS1	REELD1	RERG
RFX3-DT	RNF213-AS1	RNF223	RPAP3-DT	RPL21P28	RS1	RSPH1-DT	RUVBL1-AS1

